Geosci. Model Dev. Discuss., https://doi.org/10.5194/gmd-2017-288
Manuscript under review for journal Geosci. Model Dev.
Discussion started: 12 December 2017

Geoscientific Model Development
Open Access
Discussions

PCR-GLOBWB 2: a 5 arc-minute global hydrological and water resources model

Edwin H. Sutanudjaja[1], Rens van Beek[1], Niko Wanders[1], Yoshihide Wada[1,2], Joyce H.C. Bosmans[1], Niels Drost[3], Ruud J. van der Ent[1], Inge E. M. de Graaf[4], Jannis M. Hoch[1,5], Kor de Jong[1], Derek Karssenberg[1], Patricia López López[1,5], Stefanie Peßenteiner[6], Oliver Schmitz[1], Menno W. Straatsma[1], Ekkamol Vannametee[7], Dominik Wisser[8], and Marc F. P. Bierkens[1,9]

[1] Department of Physical Geography, Faculty of Geosciences, Utrecht University, Utrecht, The Netherlands

[2] International Institute for Applied Systems Analysis, Laxenburg, Austria

[3] Netherlands eScience Center, Amsterdam, The Netherlands

[4] Chair or Environmental Hydrological Systems , University of Freiburg, Freiburg, Germany,

[5] Unit Inland Water Systems, Deltares, Delft, the Netherlands

[6] Department of Geography and Regional Science, University of Graz, Graz, Austria

[7] Department of Geography, Chulalongkorn University, Bangkok, Thailand

[8] Center for Development Research, University of Bonn, Bonn, Germany

[9] Unit Soil and Groundwater Systems, Deltares, Utrecht, The Netherlands

Correspondence to: E. H. Sutanudjaja (E.H.Sutanudjaja@uu.nl)

Abstract.

We present PCR-GLOBWB 2, a global hydrology and water resources model. Compared to previous versions of PCR-GLOBWB, this version fully integrates water use. Sector-specific water demand, groundwater and surface water withdrawal, water consumption and return flows are dynamically calculated at every time step and interact directly with the simulated hydrology. PCR-GLOBWB 2 has been fully rewritten in Python and PCRaster-Python and has a modular structure, allowing easier replacement, maintenance, and development of model components. PCR-GLOBWB 2 has been implemented at 5 arc-minute resolution, but a version parameterized at 30 arc-minute resolution is also available. Both versions are available as open source codes on https://github.com/UU-Hydro/PCR-GLOBWB_model. PCR-GLOBWB 2 has its own routines for groundwater dynamics and surface water routing. These relatively simple routines can alternatively be replaced by dynamically coupling PCR-GLOBWB 2 to a global two-layer groundwater model and 1D-2D-hydrodynamic models, respectively. Here, we describe the main components of the model, compare results of the 30 arc-minute and the 5 arc-minute versions and evaluate their model performance using GRDC discharge data. Results show that model performance of the 5 arc-minute version is notably better than that of the 30 arc-minute version. Furthermore, we compare simulated time series of total water storage (TWS) of the 5 arc-minute model with those observed with GRACE, showing similar negative trends in areas of prevalent groundwater depletion. Also, we find that simulated water withdrawal, by source and sector, matches reasonably well with reported water withdrawal from AQUASTAT.

Geosci. Model Dev. Discuss., https://doi.org/10.5194/gmd-2017-288
Manuscript under review for journal Geosci. Model Dev.
Discussion started: 12 December 2017

1 Introduction

The last decades saw the development of an increasing number of global hydrological models (GHMs), e.g. VIC (Liang et al., 1994; Nijssen et al., 2001), WMB (Fekete et al., 2002), WaterGAP (Döll et al., 2003), H08 (Hanasaki et al., 2008a), MAC-PDM (Gosling and Arnell, 2011) (see Bierkens et al., 2014, Bierkens, 2015 and Kauffeldt et al. 2016 for a more extensive list, also including land surface models). GHMs have become essential tools to quantify and understand the global terrestrial water cycle, as they simulate the distributed hydrological response to weather and climate variations at higher resolution (typically $0.5^{o} \times 0.5^{o}$) than used previously in general circulation models (GCMs), with more sophisticated runoff generation processes and river routing. As such, global hydrological models have been used for medium-range to seasonal flood forecasting (Bierkens and van Beek, 2009; Alfieri et al., 2013; Candogan Yossef et al., 2013) as well as for a myriad of water-related global change assessments. Examples are: the projection or estimation of future flood and drought events (Sperna-Weiland et al., 2012; Dankers et al., 2013; Prudhomme et al., 2013, Wanders et al. 2015, Wanders and Wada, 2016), current and future flood hazard and risk (Pappenberger et al., 2012; Hirabayashi et al., 2013; Ward et al., 2013; Winsemius et al., 2013; 2016), global groundwater depletion (Wada et al., 2010; Gleeson et al., 2012), the contribution of terrestrial water stores to global sea level change (Konikow, 2011; Wada et al., 2012; Pohkrel et al., 2013), current and future water scarcity under climate change and increasing population growth (Hanasaki et al., 2008b; Wada et al., 2011a, 2011b; Schewe et al., 2013; Haddeland et al., 2013; Wada and Bierkens, 2014), tele-connections between climate oscillations and water availability (Wanders and Wada, 2015), the impact of land use change om global water resources (Rost et al., 2008; Sterling et al., 2015; Bosmans et al., 2016) and trends in surface water temperature and cooling water potential (van Beek et al., 2012; van Vliet et al., 2012). More recently, the output from global hydrological models has been extended to study socioeconomic impacts, such as virtual water trade (Konar et al., 2013; Dalin et al., 2017) and future agricultural production (Elliott et al., 2013). These applications show that GHMs have become invaluable tools in support of global water management and policy assessments.

PCR-GLOBWB (PCRaster GLOBal Water Balance) (van Beek and Bierkens, 2009; van Beek et al. 2011) is one of the recently developed GHMs. PCR-GLOBWB is a grid-based global hydrological model developed at the Department of Physical Geography, Faculty of Geosciences, Utrecht University, the Netherlands. The model, describing the terrestrial part of the hydrological cycle, was first introduced in a technical report by van Beek and Bierkens (2009) and then formally published in a paper of Van Beek et al. (2011), focusing on global water availability issues. PCR-GLOBWB was originally developed to solve the global daily surface water balance with a spatial resolution of 30 arc-minutes (about 50 km by 50 km at the equator) and compare the resulting fresh water availability with monthly sectoral water demand in order to assess global-scale water scarcity (van Beek et al., 2011; Wada et al., 2011a,b). In this first version of PCR-GLOBWB (called PCR-GLOBWB 1 hereafter), similar to other global-scale hydrological models, water demand and water availability are treated independently, i.e. without direct feedback between human water use and other terrestrial water fluxes (e.g. Döll and Siebert, 2002; Wisser et al., 2010). Since it was first introduced, PCR-GLOBWB has been applied extensively in global water resources assessment studies. For instance, a recent search on Scopus (accessed on 30 October 2017) on the key-word "PCR-GLOBWB" yielded 97 publications with collectively over 2100 references. Since the first version, several new model features have been introduced such as a comprehensive water demand and irrigation module (Wada et al., 2011b, 2014), a scheme for dynamic allocation of sectoral water demand to available surface water and groundwater resources and the associated calculation of return flow (de Graaf et al., 2014). These features essentially introduced a two-way interaction between water demand, water withdrawal, water consumption and availability, particularly over irrigated areas where water demand is large and return flow is significant. Nevertheless, all of these preceding studies using PCR-GLOBWB were performed at a relatively coarse resolution of 30 arc-minutes, limiting their sub-regional or local applications. Additionally, some added functionalities, such as the possibility to couple the land surface component of PCR-GLOBWB to a global MODFLOW-based groundwater model (Sutanudjaja et al., 2011; 2014; de Graaf et al., 2015; 2017) and an extension to simulate surface water temperature (Van Beek et al., 2012), were incorporated in different versions based on the original PCR-GLOWB 1, leading to divergent model code development.

The objective of this paper is to summarize and present the new version of the model, PCR-GLOBWB 2, which consolidates all components that have been developed since the original version of the model was first introduced (van Beek et al., 2011). The new version of the model, PCR-GLOBWB 2, simulates the water balance at a finer spatial resolution of 5 arc-minutes and supersedes the original PCR-GLOBWB 1 that has a resolution of 30 arc-minutes[1]. The finer resolution of PCR-GLOBWB 2 allows a much better representation of the effects of spatial heterogeneity in topography, soils, and vegetation on terrestrial hydrological dynamics (Wood et al., 2011; Bierkens et al., 2014). Likewise, it provides a better resolution for visualization that allows stakeholders and decision makers to assess model simulation output more easily and directly for the places they are specifically interested in (Sheffield et al., 2010; Beven and Cloke, 2012). To evaluate the possible improvements, this paper also presents the first validation results from the simulation of PCR-GLOBWB 2 at 5 arc-minute resolution and compares this with a 30 arc-minutes version. As discharge data are commonly used in hydrological model performance evaluation, the simulated river discharge of PCR-GLOBWB 2 is compared to in situ discharge observations from the Global Runoff Data Centre (GRDC, 2014).

The paper is organized as follows. Section 2 provides a global description of PCR-GLOBWB 2, including its model structure and the new components and functionalities that have been added since PCR-GLOBWB 1. In section 3 the global application of PCR-GLOBWB 2 is demonstrated and the results from a 58-year simulation (1958-2015) are validated against observations of discharge, total water storage and reported withdrawal data. Section 4 summarizes and concludes this paper and discusses possible future developments. Section 5 provides information about availability of the model code and the underlying data.

[1] Note that Wada et al. (2016) made a preliminary version of the model that operates at 6 arc-minutes.

2. PCR-GLOBWB 2 – Model description

2.1 General overview

PCR-GLOBWB 2 is a state-of-the-art grid-based global hydrology and water resources model. It is a component-based model implementation in Python using open source PCRaster Python routines (Karssenberg et al., 2010; http://pcraster.geo.uu.nl/). The code is distributed through Github. The computational grid covers all continents except Greenland and Antarctica. Currently two versions are available: one with a spatial resolution of 5 arc-minutes in latitude and longitude and one with a coarser resolution of 30 arc-minutes. Typical time steps for hydrology and water use are one-day while sub-daily time stepping is used for hydrodynamic river routing. For all dynamic processes involved, PCR-GLOWB 2 uses a time-explicit scheme. For each grid cell and each time step, PCR-GLOBWB 2 simulates moisture storage in two vertically stacked upper soil layers (S_1+S_2 in Figure 1), as well as the water exchange between the soil, the atmosphere and the underlying groundwater reservoir (S_3 in Figure 1). The exchange with the atmosphere comprises of precipitation, evaporation from soils, open water, snow and soils and plant transpiration, while the model also simulates snow accumulation and snowmelt. Sub-grid variability of land use, soils and topography is included and influences the schemes for runoff-infiltration partitioning, interflow, groundwater recharge (from S_2 to S_3) and capillary rise (from S_3 to S_2). Runoff, generated by snowmelt, surface runoff, interflow and baseflow, is routed across the river network to the ocean or endorheic lakes and wetlands. Routing can either be simple accumulation, simplified dynamic routing using a method of characteristics, or kinematic wave routing. In case the kinematic wave routing is used, it is also possible to use a (simplified) floodplain inundation scheme and to simulate the surface water temperature.

PCR-GLOBWB 2 includes a simple reservoir operation scheme that is applied to over roughly 6000 manmade reservoirs from the GranD database (Lehner et al., 2011), which are progressively introduced according to their construction year. Human water use is fully integrated within the hydrological model, meaning that at each time step: 1) water demands are estimated for irrigation, livestock, industry and households; 2) these demands are translated into actual withdrawals from groundwater, surface water (rivers, lakes and reservoirs) and desalinization, subject to availability of these resources and maximum groundwater pumping capacity in place; 3) consumptive water use and return flows are calculated per sector.

As an option PCR-GLOBWB 2 can be partially or fully coupled to a two-layer global groundwater model based on MODFLOW (de Graaf et al, 2017). Recent work (Hoch et al., 2017a,b) also includes coupling PCR-GLOBWB 2 to either Delft3D Flexible Mesh (Kernkamp et al., 2011) or LISFLOOD-FP (Bates et al., 2010) which are model codes that can be used to solve the 1D-2D shallow water equations (or approximation thereof) for detailed inundation studies.

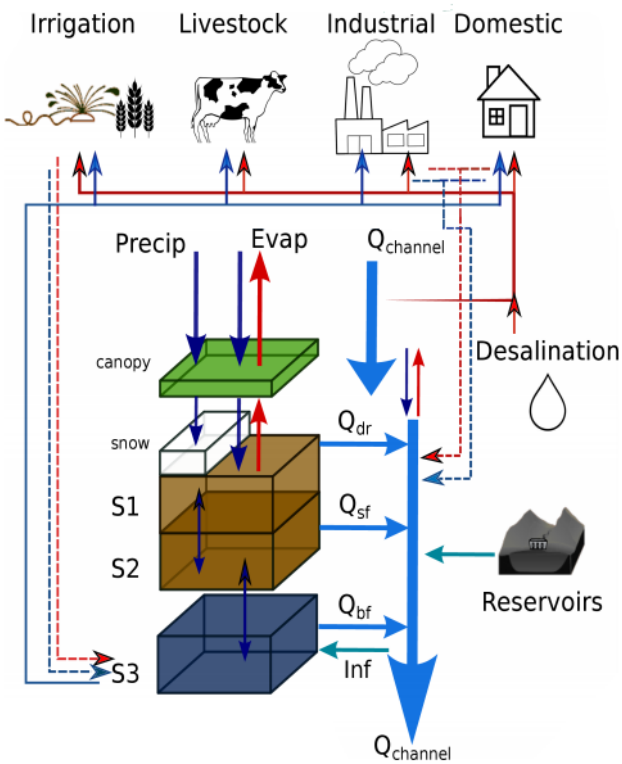

Figure 1. Schematic overview of a PCR-GLOBWB 2 cell and its modelled states and fluxes. S_1, S_2 *(soil moisture storage),* S_3 *(groundwater storage),* Q_{dr} *(surface runoff – from rainfall and snowmelt),* Q_{sf} *(interflow or stormflow),* Q_{bf} *(baseflow or groundwater discharge),* Inf *(riverbed infiltration from to groundwater). The thin red lines indicate surface water withdrawal, the thin blue lines groundwater abstraction, the thin red dashed lines return flows from surface water use and the thin dashed blue lines return flows from groundwater use surface. For each sector: withdrawal - return flow = consumption. Water consumption adds to total evaporation.*

Geosci. Model Dev. Discuss., https://doi.org/10.5194/gmd-2017-288
Manuscript under review for journal Geosci. Model Dev.
Discussion started: 12 December 2017

Geoscientific Model Development Discussions
Open Access

2.2 Model structure and flexibility

PCR-GLOBWB 2 has a flexible modular structure in which the exchange of water between a series of interconnected stores is easily performed (Figure 1). The modular structure of PCR-GLOBWB 2, both in terms of model concepts and implementation (separate modules are called from a main program), makes it easy to modify or replace components according to specific objectives of the model application, to introduce new modules or components within the modelling system and to couple it to existing codes.

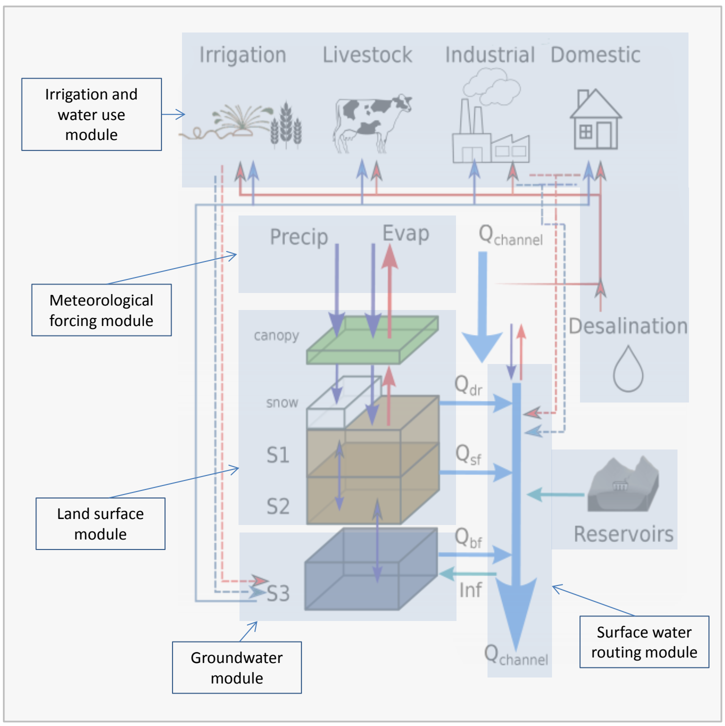

Figure 2. The five modules that make up PCR-GLOBWB 2 portrayed on the model components of Figure 1.

There are currently five main hydrological modules in PCR-GLOBWB 2 as illustrated in Figure 2 and briefly described in Section 2.3: Meteorological forcing; Land surface; Groundwater; Surface water routing; Irrigation and water use. For an extensive description of the underlying equations and methods used in each of these modules we refer to the following sources:

- Meteorological forcing module: van Beek (2008) http://vanbeek.geo.uu.nl/suppinfo/vanbeek2008.pdf
- Land surface module, groundwater module and surface water routing module: van Beek and Bierkens (2009) http://vanbeek.geo.uu.nl/suppinfo/vanbeekbierkens2009.pdf ; van Beek et al. (2011) http://dx.doi.org/10.1029/2010WR009791
- Irrigation and water use module:
  - Calculation of water demand: Wada et al., (2014) https://doi.org/10.5194/esd-5-15-2014
  - Calculation of water withdrawal, consumption and return flows: de Graaf et al. (2014) https://doi.org/10.1016/j.advwatres.2013.12.002; Wada et al. (2014) https://doi.org/10.5194/esd-5-15-2014; Erkens and Sutanudjaja (2015) https://doi.org/10.5194/piahs-372-83-2015

Furthermore: for details about coupling to MOFLOW we refer to:

- One-way coupling: Sutanudjaja et al. (2011) https://doi.org/10.5194/hess-15-2913-2011; De Graaf et al. (2017) https://doi.org/10.1016/j.advwatres.2017.01.011
- Two-way coupling: Sutanudjaja et al. (2014) http://dx.doi.org/10.1002/2013WR013807

2.3 Description of the modules

Hereafter, we briefly describe the main features of the five modules. Additionally, a (non-exhaustive) list of the model state and flux variables is provided in Table A1, whereas Table A2 lists the model inputs and parameters, including their sources.

2.3.1 Meteorological forcing module

Meteorological forcing of PCR-GLOBWB 2 uses time series of spatial fields of precipitation, temperature and reference evaporation. Reference potential evaporation can be prescribed or calculated within the model, and is used in the land surface module to calculate crop-specific potential evaporation based on crop factors of the various land cover types according to the FAO guidelines (Allen et al., 1998). There are two options for calculating reference potential evaporation: 1) using Hamon (1963) in case only daily mean temperature is available; 2) using Penman-Monteith following the FAO guidelines (Allen et al., 1998) if net radiation, wind speed and vapour pressure deficit are additionally available. See van Beek et al. (2008) for details. The resulting crop specific potential evaporation is subsequently used to compute the actual evaporation for different land cover types in each cell. Apart from the calculation of evaporation, temperature is also used to partition precipitation into snow and rain and to drive snowmelt.

2.3.2. Land surface module

This core module of PCR-GLOBWB 2 covers the land-atmosphere exchange, the vertical flow between soil compartments and the eventual groundwater recharge, snow and interception storage and the runoff generation mechanisms. Information is organized per land cover type and the fraction it occupies within a cell. The number of land cover types is configurable; the standard parameterization of PCR-GLOBWB 2 carries: tall natural vegetation, short natural vegetation, irrigated crops (non-paddy) and paddy-irrigation (i.e., wet rice). For each land cover type, separate soil conditions can be specified. It should be noted that the soil and vegetation conditions are in any case fully spatially distributed. Thus, vegetation properties (e.g., crop factor, Leaf Area Index) and soil properties (depth, saturated hydraulic conductivity, etc.) vary not only between land cover types, but may also vary from cell-to-cell (e.g., per climate zone). In the standard parameterization vegetation properties vary over the year using a monthly climatology of phenology and crop calendars (i.e. for the crop factor and LAI). The application of irrigation water for paddy and non-paddy irrigation is done by the irrigation and water use module. It is based on the FAO guidelines of Allen et al. (1998) and is dependent on the actual soil water storage (S_1, S_2) or paddy-open water storages. All fluxes, from and to the land surface module in Figure 2, are thus calculated separately per land cover type. The resulting vertical fluxes for each land cover type are: interception evaporation, bare soil evaporation, snow sublimation, vegetation-specific transpiration. In the soil column, vertical fluxes are based on Darcian flow and interact with the underlying groundwater store, S_3. Surface runoff (Q_{dr}, from precipitation and snowmelt) consists of infiltration excess runoff and saturation excess runoff following a sub-grid approach that mimics variable source areas, i.e. the improved Arno Scheme (Todini, 1996; Hagemann and Gates, 2003). Interflow or stormflow (Q_{sf}), mostly occurring in regolith soils on hillslopes, is also handled with a sub-grid approach based on a runoff parameterization by Sloan and Moore (1984). All fluxes are computed per land cover type and balanced with the available storage to arrive at the net flux that is used to update the storages for the next time step. Also, to report the overall fluxes per cell, and to pass these to other modules, the land cover specific fluxes are subsequently averaged (weighted by land cover type fractions).

For the standard parameterization of the land surface module the following data sets are combined (see Table A2): the cell fractions of various non-irrigation land cover types are based on the map of Global Land Cover Characteristics Data (GLCC) Base Version 2.0 (Loveland et al., 2000) with the land cover classification following Olson (1994a; b) and the parameter sets from Hagemann et al. (1999) and Hagemann (2002). Irrigation land cover types (i.e. paddy and non-paddy), including their crop calendars and growing season lengths, are parameterized based on the data set of MIRCA2000 (Portmann et al., 2010) and the Global Crop Water Model of Siebert and Döll (2010). We refer to van Beek et al. (2011) for detailed descriptions.

2.3.3. Groundwater module

The groundwater module calculates groundwater storage dynamics subject to recharge and capillary rise (calculated by the land surface module), groundwater discharge (Q_{bf}; in case of a positive groundwater storage) and riverbed infiltration (Inf). Groundwater discharge (assumed the same as groundwater baseflow here) depends on a linear storage-outflow relationship ($Q_{bf} = S_3/J$) where the proportionality constant J is calculated following drainage theory of Kraijenhoff-van de Leur (1958) based on drainage network density and aquifer properties. Riverbed infiltration occurs only in case Q_{bf} becomes 0 by groundwater withdrawal, and only in areas where under natural conditions (without groundwater withdrawal) significant groundwater discharge occurs. Under persistent groundwater withdrawal (calculated with the Irrigation and Water use module) that is larger than the sum of recharge and riverbed infiltration, the groundwater storage S_3 is allowed to become negative. In this case, the part of the withdrawn groundwater in excess of the input (recharge and riverbed infiltration) is seen as non-renewable groundwater withdrawal leading to groundwater depletion (permanent loss of groundwater from storage). In case withdrawal becomes smaller than the input, the remaining input is used to first fill the negative storage to zero, before baseflow Q_{bf} commences again. Alternatively, an initial estimate of a fossil, i.e. a non-actively replenished, groundwater store can be imposed that provides a similar functionality.

It is possible to use a full-fledged groundwater flow model based on MODFLOW: Harbaugh et al., 2000) coupled to PCR-GLOBWB 2 in order to calculate groundwater heads and flow paths. This can be done as a one-way coupling where PCR-GLOWB 2 is first run with the standard groundwater module (reservoir S_3 with only vertical fluxes) to yield time series of net groundwater recharge (recharge – capillary rise) and surface water levels. These fluxes/inputs are subsequently used to force the groundwater flow model (see e.g. Sutanudjaja et al., 2011; de Graaf et al., 2017). Another possibility is to use a two-way coupling where the groundwater module of PCR-GLOBWB 2 is replaced by the groundwater flow model. In this case, at each time step fluxes are exchanged between the groundwater model and the land surface module, and the groundwater model and the surface water routing module (Sutanudjaja et al. 2014).

2.3.4 Surface water routing module

Following an 8-point steepest gradient algorithm across the terrain surface (local drainage direction or LDD), all cells of the modelled domain are connected to a strictly convergent drainage network that together make up the river basins and sub-basins of the model domain. The lowermost cell is either connected to the ocean or to an endorheic basin. Per cell, the sum of the three daily runoff fluxes (Figure 1) is aggregated and routed along the drainage network. Routing can be done in three ways of increasing complexity: 1) accumulation of the fluxes over the drainage network, typically aggregated over longer time steps (e.g. month or year) that are larger than the travel times of water along the longest river length; 2) a travel-time characteristic solution (Karssenberg et al., 2007). Here, for each cell flow velocity is calculated in advance based on bankfull discharge and Manning's equation (assuming the energy slope to be equal to the bed slope). Next, this velocity is used to move the volume of water in the channel of a cell the corresponding distance within one time step along the drainage network. This method works reasonably well for relatively steep rivers in humid climates where the friction slope is close to the bed slope and the rivers are equally filled with water throughout the year; 3) the kinematic wave approximation of the Saint Venant equations with flow described by Manning's equation. Also, here, it is assumed that friction slope and bed slope are equal, which makes it valid for rivers without backwater effects. The kinematic wave is solved using a time-explicit variable sub-time stepping scheme based on the minimum Courant number. Of these methods, the kinematic wave solution simulates the propagation of the flood wave more realistically while the others provide an expedient means to approximate discharge over longer periods.

Using the kinematic wave method, it is possible to model floodplain inundation which occurs if the discharge exceeds the bankfull capacity of a channel. The excess discharge volume is spread over the entire cell from the lowest part of the cell (based on a higher resolution sub-grid DEM) yielding a flooded area with an approximated flood depth. In case of flooding, the simulated river flow is impacted by adjusting the wetted area and wetted perimeter and calculating a weighted Manning coefficient from the individual Manning coefficients of the floodplains and the channel.

Lakes and reservoirs are part of the drainage network. Lakes and reservoirs can extend over multiple cells, in which case the storage is subdivided by area such as to ensure that lake and reservoir levels are the same across their extent. The active storage of lakes and the actual storage of reservoirs are dynamically updated; for the lake outflow a standard storage-outflow relationship is used based on a rectangular cross-section over a broad-crested weir, while reservoirs follow a release strategy. This strategy is, by default, aimed at passing the average discharge, while maintaining levels between a minimum and maximum storage, but more elaborate strategies that take account of downstream water demand are possible (e.g. Van Beek et al., 2011). Lakes and reservoir areas change based on global volume-area relationships. All surface water areas, i.e. the river channel, inundated floodplains, lakes and reservoirs, are subject to open water evaporation calculated from reference potential evaporation multiplied with a factor depending on water type and water depth. Moreover, surface waters are subject to surface water withdrawal calculated with the Irrigation and Water Use module.

If the kinematic wave approach is used, it can be also augmented with an energy routing scheme to simulate surface water temperature (Van Beek et al., 2012). Finally, it should be noted that it is possible to run the routing routine from PCR-GLOBWB 2 as a stand-alone routine, which allows it to be fed with the specific discharge from other land surface models.

The routing methods that are available in PCR-GLOBWB 2 will yield significant errors for wide lowland rivers where backwater effects are important. In this case, it is possible to replace the surface water module for part of the modelling domain with hydrodynamic models solving the shallow water equations (Hoch et al., 2017a). Hoch et al. (2017b) developed a generic coupler for this purpose that enables coupling to multiple hydrodynamic modelling codes (https://doi.org/10.5281/zenodo.597107).

Although any data set can be used to define the drainage network and locate the lakes and reservoirs, the standard parameterization of PCR-GLOBWB 2 that runs globally uses the drainage network derived from HydroSHEDS (Lehner et al., 2008) combined with GTOPO30 (Gesch et al., 1999) and Hydro1k (Verdin and Greenlee, 1996; USGS EROS Data Center, 2006); lakes taken from GLWD1 (Lehner and Döll, 2004) and reservoirs obtained from GranD (Lehner et al., 2011).

2.3.5 Irrigation and water use module

In PCR-GLOWB 1 water demand was calculated separately from the hydrology and water availability calculated as a post-processing step by subtracting upstream demand (Wada et al., 2011a,b). In PCR-GLOBWB 2 water use (withdrawal and consumption) is fully integrated. Hereafter, the main features of the irrigation and water use module are described in the following order: water demand, water withdrawal, water consumption and return flows.

Water demand

Irrigation water demand is calculated based on the crop composition (which changes per month and includes multi-cropping) and the irrigated area per cell. As stated above, these are obtained from MIRCA2000 (Portmann et al., 2010) and the Global Crop Water Model (Siebert and Döll, 2010). In the standard PCR-GLOBWB 2 parameterization the irrigated areas change over time. In want of detailed data, fractions of paddy and non-paddy irrigation, as well as the crop composition per month stay fixed (as obtained from MIRCA2000), while the total irrigated area per cell changes over time and is based on the FAOSTAT (FAO, 2012) reported irrigated areas. Irrigation water demand is computed using the FAO guidelines (Doorenbos and Pruit, 1977; Allen et al., 1998): in case of non-paddy irrigation, water is applied whenever soil moisture falls below a pre-set value and then the soil column is replenished up to field capacity. In case of paddy irrigation, the water level is kept at a water depth of 5 cm above the surface until the late crop development stage (~ 20 days) before the harvest. After that, no irrigation is applied anymore such that the water level is allowed to drop to zero under infiltration and evaporation (Wada et al., 2014). The net irrigation demand is augmented to account for limited irrigation efficiency and losses. In the standard parameterization of PCR-GLOBWB the irrigation water demand is increased by 40% to obtain gross irrigation water demand (meaning an irrigation efficiency of $(1/1.4)\times100 = 71\%$.) However, it is possible to use spatio-temporal varying irrigation efficiencies if needed, which is the case for all other variables.

Non-irrigation water demand covers three sectors; industry, households and livestock. For each of these sectors, the gross demand and net demand are prescribed to the model and calculated using separate scripts. The calculation of net non-irrigation water demand, which varies with time, follows methods developed by Wada et al (2014). We refer to Wada et al. (2014) for an extensive description. Trends in water demand are prescribed on an annual basis as a function of population, electricity demand and gross domestic product (GDP) per capita. In addition, domestic water demand exhibits a seasonal variation on the basis of temperature. Domestic and industrial gross water demand is calculated from net water demand using a country-specific recycling ratio *RC* (based on development stage or GDP per capita and additionally access to domestic water demand): gross = net/(1-*RC*). This takes into account that much of the domestic and industrial water is not consumed but returned as surface water. For livestock, the return flow is assumed to be zero, meaning all water is consumed.

Water withdrawal

The water withdrawal estimation is based on the work by de Graaf et al. (2014) and Wada et al. (2014). In PCR-GLOBWB 2 water withdrawal is set equal to gross water demand (summed over all the sectors) unless sufficient water is not available. In that case, water withdrawal is scaled down to the available water and then allocated proportionally to gross water demand per sector. Thus, no allocation preference is available in the standard parameterization of PCR-GLOBWB 2, but it would be rather straightforward to change this.

Water can be abstracted from three sources: surface water, groundwater (fossil and non-fossil) and desalinated water. The latter is prescribed (Wada et al., 2011a), while the fractions of the other two sources are determined as function of their relative abundance. Groundwater and surface water availability are determined based on two-year running means of groundwater recharge and river discharge respectively, thus keeping track of the prevalence of local resources and their temporal change (de Graaf et al., 2014). These fractions determine on a monthly basis from which source water is abstracted. Surface water withdrawal is ceased if river discharge falls below 10% of the long-term average yearly discharge under naturalized flow conditions (determined by running the model without withdrawal). If, for some reason, the surface water amount is insufficient, the model falls back on groundwater to meet the resulting gap. Groundwater is first abstracted from the renewable groundwater storage, and if not this is not present, non-renewable groundwater is abstracted. The amount of groundwater that can be abstracted is, however, capped by the groundwater pumping capacity which is based on data by IGRAC GGIS database. The described dynamic allocation scheme is not always in line with local preferences or the infrastructure. However, there is a possibility to use literature fractions of groundwater withdrawal and surface water withdrawal. For urban areas, we rely on the data set of McDonald et al. (2014) that states whether a surface water distribution infrastructure is available. If this is the case, industrial and domestic water withdrawals are mainly taken from surface water before abstracting groundwater. If surface water infrastructure is limited, groundwater source is prioritized (see e.g. Erkens and Sutanudjaja, 2015). For urban areas that are not in the McDonald (2014) data set, we give preference to the dynamic allocation scheme. For irrigation, we use the ratios supplied by Siebert et al. (2010) in regions where they are said to be reliable. In regions where they are not fully reliable, we take the average ratio provided by Siebert et al. (2010) and the one provided by the dynamic allocation scheme. For regions where the data of Siebert (2010) are not reliable (i.e., extrapolated data), we give preference to the dynamic allocation scheme.

Moreover, we cannot assume that all the water demand is supplied from surface water and groundwater resources in the same cell. Ideally, the local water redistribution network should be used to define a surface water service area. Unfortunately, this information is not available at the global scale. Therefore, in our current parameterization of PCR-GLOBWB 2, we pool water availability of desalinated and surface water over zones of approximately 1 arc-degree around each 5 arc-minute cell that are truncated by country and basin borders if applicable. For groundwater, 0.5 arc-degree zones are used. The downside of the current scheme is that a cell does not always have access to its nearest water resource if this lies outside its prescribed service area. Available surface water for abstraction is stored in channels, lakes and reservoirs within each cell and service area. Groundwater availability is also limited by the pumping capacity in the service area.

Water consumption and return flows

In case of irrigation, all the withdrawn water is applied to the soil (non-paddy) or the water level on the field (paddy). Part of that water is lost by transpiration and part by soil and open water evaporation. Transpiration and evaporation together make up the irrigation water consumption. The remaining part of irrigated water is lost by percolation and contributes to groundwater recharge as return flow. Irrigation efficiency (not including conveyance losses) could also be calculated after the fact by the difference between withdrawal and transpiration. In case of domestic and industrial water use, water consumption depends on the recycling ratio RC and equals withdrawal×(1-RC), while withdrawal×RC constitutes return flow. All return flow is added to the surface water. For livestock, the consumption is set equal to the withdrawal and no return flow is assumed.

2.4 Differences between PCR-GLOBWB 1 and 2

PCR-GLOBWB 2 has the following new capabilities compared to PCR-GLOBWB 1 (cf. Van Beek et al., 2011; Wada et al, 2011):

- the model was completely rewritten in PCRaster Python and now has a modular structure;
- the inputs and outputs are in the form of NetCDF files and output can be reported for daily monthly and yearly time steps;
- parameterizations are available at 30 arc-minute and 5 arc-minute resolution;
- water use (demand, withdrawal, consumption and return flow) is fully integrated;
- distinction is made between paddy and non-paddy irrigation and irrigation follows FAO guidelines;

Geosci. Model Dev. Discuss., https://doi.org/10.5194/gmd-2017-288
Manuscript under review for journal Geosci. Model Dev.
Discussion started: 12 December 2017

Geoscientific Model Development Discussions
Open Access

- three different options for surface water routing are available and a surface water temperature module is fully integrated with the routing scheme;
- it is possible to run surface water routines separately with specific discharge from other sources (e.g. other land surface models);
- PCR-GLOBWB 2 can be coupled to a two-layer transient groundwater model (Sutanudjaja et al., 2014; De Graaf et al., 2017) and to the hydrodynamic models Delft3D Flexible Mesh (Kernkamp et al., 2011) or LISFLOOD-FP (Bates et al., 2010, see Hoch et al., 2017b).

2.5 Model code

The original PCR-GLOBWB version 1 (van Beek et al., 2011) was written in the PCRaster scripting language. PCRaster (Wesseling et al., 1996) is a high-level programming language that started as a dynamic raster-based Geographical Information System (GIS) and is tailored to spatiotemporal modelling for environmental and earth science applications. The generic nature of PCRaster with its many tailor-made built-in hydrological functions and its syntax that reads like pseudo-code, generally results in short and readable model codes, short development times and limited programming errors. Karssenberg et al. (2010) developed a PCRaster Python package such that PCRaster functions, implemented in C++, can also be called via Python (http://www.python.org/). Using PCRaster Python also makes it possible for students and beginner modellers to contribute to the model quickly, while it allows experts to be more productive and focus on the science rather than on the programming language syntax. Realising the aforementioned advantages, PCR-GLOBWB, particularly starting from this version 2, has been rewritten in the Python scripting language.

To run the model a so-called initialization file or configuration file is used (with extension .ini). In this file the following aspects are defined: the spatial and temporal domain, the time step, the settings of the different modules (e.g. which surface water routing, human water use or not etc.) and the locations and names of the parameter files and forcing files. As mentioned above, PCR-GLOBWB 2 uses NetCDF files for most input and all output, thus making it easier to exchange data with other scientists and use existing tools to analyse its output.

PCR-GLOBWB 2 generally runs under Linux. It is also possible to run it under Windows, but Windows memory constraints limit domain size and time steps simulated. In order to run PCR-GLOBWB the following additional software needs to be installed: PCRaster version 4, Python versions 2.7 with Python packages numPy and netCDF4 and gdal version 1.8 or higher.

3. Model demonstration and evaluation

To test and evaluate the performance of PCR-GLOBWB 2, we ran the model at both 30 arc-minute and 5 arc-minute resolution over the period 1958-2015. We compared the results of both simulations with discharge data from the GRDC Global Runoff Data Centre (GRDC, 2014), with total basin water storage estimates from GRACE (Gravity Recovery and Climate Experiment; Wiese, 2015) and with water withdrawal data from the FAO AQUASTAT database (FAO, 2016).

3.1 Model run setup

3.1.1 Parameterization

We used the standard parameterization (parameters, forcing and their sources in Table A2) of PCR-GLOBWB 2 at 30 arc-minute and 5 arc-minute spatial resolutions to simulate global hydrology at daily resolution over 1958-2015. Outputs were reported as monthly averages. Note that parameterizations were derived directly following their source data sets using hydrological concepts described in Van Beek and Bierkens (2009). We stress that no calibration was performed. We ran the model with human water use options on and used the travel-time characteristic solution routing option.

3.1.2 Forcing

The forcing data set is based on time series of monthly precipitation, temperature and reference evaporation from the CRU TS 3.2 data set of Harris et al. (2014) downscaled to daily values with ERA40 (1958-1978; Uppala et al., 2005) and ERA-Interim (1979-2015; Dee et al., 2011). CRU is specified at 30 arc-minute spatial resolution and directly usable. We used ERA40 and ERA-I results that had been resampled by ECMWFs resampling scheme from their original resolutions (~1.2º and ~0.7º) to 30 arc-minutes first. Precipitation was temporally downscaled by first applying a threshold of 0.1 mm/day to the ERA daily time series to estimate the number of rain days for ERA. The amount of rainfall below this threshold was proportionally allocated to the rain days. Next, the daily rainfall totals were scaled in order to reproduce the CRU monthly precipitation total using multiplicative scaling. Equally, monthly reference potential evaporation, computed with Penman-Monteith from the CRU data set was scaled using multiplicative scaling and downscaled to daily data proportional to Hamon (1967) evaporation calculated from daily ERA temperatures. For the air temperature, an additive scaling factor was used. To better simulate snow-dynamics for the 5-arc-minute model, the temperature values from CRU were further spatially downscaled to 5 arc-minutes using a temperature lapse-rate derived from the higher-resolution CRU V1.0 climatology (New et al., 2002). For areas where the number of stations underlying the CRU data set was found to be small, preference was given to using directly the meteorological data from ERA. The method used to create the forcing data set is described more extensively in Van Beek (2008).

3.1.3 Spin-up

The large groundwater response times for certain regions (e.g. Niger and Amazon) requires substantial spin-up for the groundwater volumes to be in equilibrium with the current climate. To reach this equilibrium, the model was spun-up using the average climatological forcing over the years 1958–2000 back-to-back for 150 years to reach a dynamic steady state. This spin-up was executed under naturalized condition which means no reservoirs and no human water use.

3.1.4 Computation time and parallelization

The models were run on Cartesius, the Dutch national supercomputer (https://userinfo.surfsara.nl/systems/cartesius). Without parallelization, the wall clock time for a one-year global simulation run of the 30 arc-minute model was about one hour. This entails that a one-year global simulation run with the 5 arc-minute model, might result in wall clock times at least 36 hours. Hence, to speed-up computation, the 5 arc-minute model domain was divided into 53 groups of river basins such that it could be run as 53 separate processes. With this simple parallelization technique, the wall clock time for a one-year simulation run of the 5 arc-minute model reduced to about one hour again. Note that these computation times were obtained for simulations with the travel-time characteristic routing option. Calculation times would have been significantly longer if the kinematic wave routing had been used (e.g. about 6 hours for a one-year 5 arc-minutes global run including parallelization).

3.2 Data used for comparison

3.2.1 River discharge

We used discharge stations from GRDC (2014) to compare simulated discharge from PCR-GLOBWB 2 with monthly reported discharge. From all the globally available stations in the database, we selected a subset of stations using the following criteria: 1) allowing a not more than 15% difference in catchment area between PCR-GLOBWB 2 and the area reported with the GRDC discharge station; 2) not more than 1 cell distance between the station location and the nearby location of a main river in PCR-GLOBWB 2; 3) at least 1 year of discharge data. This yielded 5363 stations for the 5 arc-minute simulation, 3910 stations for the 30 arc-minute simulation and 3597 stations fulfilling the criteria for both resolutions. As we jointly compared the performance of both simulations, we used the set of 3597 locations throughout. The average time series length of these stations is equal to 36 years.

3.2.2 Total water storage

We compared total water storage (TWS) as simulated by PCR-GLOBWB 2 with the TWS estimated from GRACE (Gravity Recovery and Climate Experiment) gravity anomalies. We used the GRACE JPL Mascon product PL-RL05M (Wiese, 2015; Watkins et al., 2015; Wiese et al., 2016). Scanlon et al. (2016) suggest that recent developments in mascon (mass concentration) solutions for GRACE have significantly increased the spatial localization and amplitude of recovered terrestrial TWS signals. They also claim that one of the advantages of using the mascon solutions relative to traditional SH (spherical harmonic) solutions is that it makes it much easier for non-geodesists to apply GRACE data to hydrologic problems. Note that although the data of PL-RL05M are represented on a 30 arc-minutes lat-lon grid, they represent the 3x3 arc-degree equal-area zones, which is the actual resolution of JPL-RL05M. We compared trends on a pixel-by-pixel basis. Given the coarse resolution of GRACE products of about 300 km by 300 km we compared cross-correlations only for major river basins with an area of 900,000 km^2 and up.

3.2.3 Water withdrawal

The water withdrawal for a large number of countries is taken from FAO's AQUASTAT database (FAO, 2016) This data is on average reported in every 5 years. We compared simulated water withdrawal per sector and per water source (surface water and groundwater) with reported values per country and per reporting period, whenever available.

3.3 The global water balance simulated at 30 and 5 arc-minutes

We calculated the main global water balance components from the 30 arc-minute and 5 arc-minute simulations over the period 2000-2015. The results in Table 1 show that there are some differences between the two model runs, but values are in the same order of magnitude. The small difference in precipitation is due to the fact that the area of the land cells is slightly different at the two resolutions. Differences in evaporation and runoff show that the runoff and evaporation parameterization of PCR-GLOBWB 2 is not entirely scale-consistent. Differences in evaporation may also be causing the

Geosci. Model Dev. Discuss., https://doi.org/10.5194/gmd-2017-288
Manuscript under review for journal Geosci. Model Dev.
Discussion started: 12 December 2017

differences in irrigation water demand which in turn may explain the differences in water withdrawal. Recently, Samaniego et al. (2017) applied their multiscale parameter regionalization (MPR) technique to PCR-GLOBWB 2 for the Rhine basin, showing that scale-consistent flux-preserving parameterisation is possible. However, a global application of this method to all PCR-GLOWB 2 parameters is not possible yet. Nonetheless, when comparing the results of both model runs with data reported in the literature, it shows that the global water balance components are similar to recent assessments (e.g. by Rodell et al., 2015) and groundwater withdrawal and total withdrawal estimates match those of previous studies (see Table 2).

From Table 1, it can also be seen that there is a negative change in total terrestrial water storage in both model runs. Table 1 shows that this can only be partly explained by groundwater depletion, which is localized to certain regions (see also Sect. 3.4.2). Further analysis shows that this change can also be attributed to the trends in precipitation forcing used, particularly over the tropics.

Table 1. Global Water balance components and human water withdrawal (in km^3/year) over the period 2000-2015 as obtained from the 30 arc-minutes and the 5 arc-minute simulations. The numbers are shown to high significance to show the water balance closure. This does not mean that we pretend to know e.g. global discharge with a km^3 accuracy (actual accuracy of the large fluxes is more in the order of 10^3 km^3)

		30 arc-min (km^3/year)	5 arc-min (km^3/year)
Global water balance	Precipitation	107452	107495
	Desalinated water use	3	2
	Runoff	42393	43978
	Evaporation*	65754	63974
	Change in total water storage	-693	-455
Groundwater budget	Groundwater recharge	27756	25521
	Groundwater withdrawal	737	632
	Non-renewable groundwater withdrawal (groundwater depletion)	173	171
	Renewable groundwater withdrawal	564	460
Withdrawal by sector	Agricultural water withdrawal (irrigation + livestock)	2735	2309
	Domestic water withdrawal	380	314
	Industrial water withdrawal	798	707
Withdrawal by source	Total water withdrawal	3912	3330
	Surface water withdrawal	3172	2697
	Desalinated water use	3	2
	Groundwater withdrawal	737	632

* Includes consumptive water use for livestock, domestic and industrial sectors

Geosci. Model Dev. Discuss., https://doi.org/10.5194/gmd-2017-288
Manuscript under review for journal Geosci. Model Dev.
Discussion started: 12 December 2017

Table 2. Groundwater withdrawal (a) and total water withdrawal (b) as compared to other studies

a) Groundwater withdrawal

Source	Year	Value (km^3/year)
Döll et al. (2012)	1998-2002	571
Döll et al. (2014) (their Table 2).	2003-2009	690-888
Döll et al. (2014) (their Table 6).	2000-2009	665
Pokhrel et al. (2015)	1998-2002	570 (±61)
Wada et al. (2010) (from the IGRAC database)	2000	734 (±87)
This study (5 arc-minutes)	2000-2015	632

b) Total water withdrawal

Source	Year	Value (km^3/year)
Döll et al. (2012)	1998-2002	4340
Döll et al. (2014) (their Table 2)	2003-2009	3000-3700
FAO (2016)	2010	3583
Oki and Kanae (2006): 3800 km3/year (contemporary)	2006	3800
Vörösmarty et al. (2005)	1995-2000	3560
This study (5 arcminutes)	2000-2015	3330

3.4 Evaluation of the 30 and 5 arc-minute simulations

3.4.1 Discharge

When evaluating the simulated discharge with discharge observations from GRDC we calculated three different measures: 1) the cross-correlation coefficient between simulated and observed GRDC time series, which is a measure of reproducing correct timing of high and low discharge. A correlation coefficient of 1 is perfect timing; 2) the Kling-Gupta efficiency coefficient or KGE (Gupta et al., 2009) which equally measures bias, differences in amplitude and differences in timing. The KGE varies between 1 and minus infinity, where 1 means a perfect fit in terms of bias, amplitude and timing; 3) anomaly cross-correlation, i.e. the cross-correlation between time series after the seasonal signal (climatology) has been removed. This statistic measures the ability of the model to correctly simulate timing of seasonal and the inter-annual anomalies from the yearly climatology. It shows if the model is capable of capturing hydrological extremes and is not only driven by the climatology. An anomaly correlation of 1 indicates perfect characterization of the extremes and values below 0 indicates a lack thereof.

Figure 3 shows maps of the cross-correlation coefficients for the GRDC stations considered and Figure 4 shows histograms of cross-correlation and KGE values. Both figures show that the validation results of the 5 arc-minute simulation are notably better than those of the 30 arc-minute simulation. For the 30 arc-minute model the number of catchments with KGE > 0, 0.3 and 0.6 are equal to 48%, 26% and 7% of the total catchments respectively. For the 5 arc-minute model these values are respectively equal to 63%, 40% and 12% of the total catchments. Note that for both runs the standard parameterization was used. Possible explanations for the better performance of the 5 arc-minute run are: a better delineation of the outline of the basins, particularly the smaller ones, a better characterization of basin relief and the drainage network, more accurate sub-grid parameterization of soil and land cover due to a smaller scale-gap that needs to be overcome, better estimates of the basin storage and better snow dynamics due to the downscaling of temperature to 5 arc-minute resolution. The KGE values are less favourable than the cross-correlation coefficients. This is mostly due to biases in runoff caused by to incorrect meteorological forcing.

The maps of cross-correlations (Figure 3) show the best results in Europe and North America where the meteorological forcing is generally more accurate as a result of more data used in the re-analysis products and higher station availability in the CRU data set. Also, monsoon-dominated basins are well simulated due to the strong seasonal nature of both forcing and related discharge. The improvement of the 5 arc-minute simulation over the 30 arc-minute simulation in Europe is mostly seen in the Alps and the Norwegian mountains. This reflects the fact that topography and thus snow dynamics is better represented at higher resolution. The least accurate results are obtained for some of the African rivers, in particular the Niger where the groundwater recession constants are probably over-estimated and inland delta evaporation is under-estimated, and for some rivers in the Rocky Mountains, which may be the result of errors in snow dynamics. Although results are generally better, the spatial distribution of results is similar to those found by Van Beek et al. (2011) for PCR-GLOBWB 1. The histograms of validation results in Figure 4 do not show a strong relationship between catchment size and validation statistics. This suggests that the improvements of model results equally apply to all catchment sizes when moving from a coarser to higher resolution.

Geosci. Model Dev. Discuss., https://doi.org/10.5194/gmd-2017-288
Manuscript under review for journal Geosci. Model Dev.
Discussion started: 12 December 2017

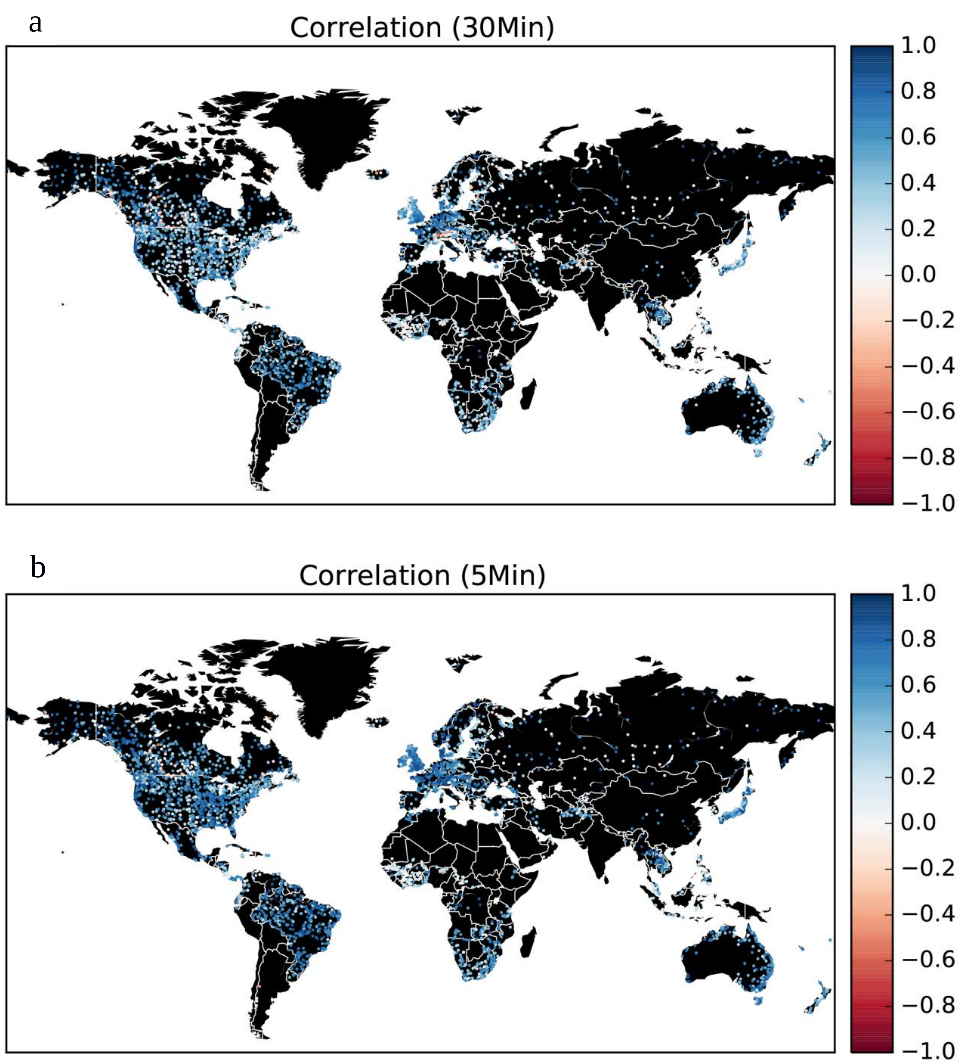

Figure 3 Maps of cross-correlation between simulated and observed discharge time series for 3597 GRDC discharge stations; a. results for the 30 arc-minute simulation; b. results for 5 arc-minute simulation.

Geosci. Model Dev. Discuss., https://doi.org/10.5194/gmd-2017-288
Manuscript under review for journal Geosci. Model Dev.
Discussion started: 12 December 2017

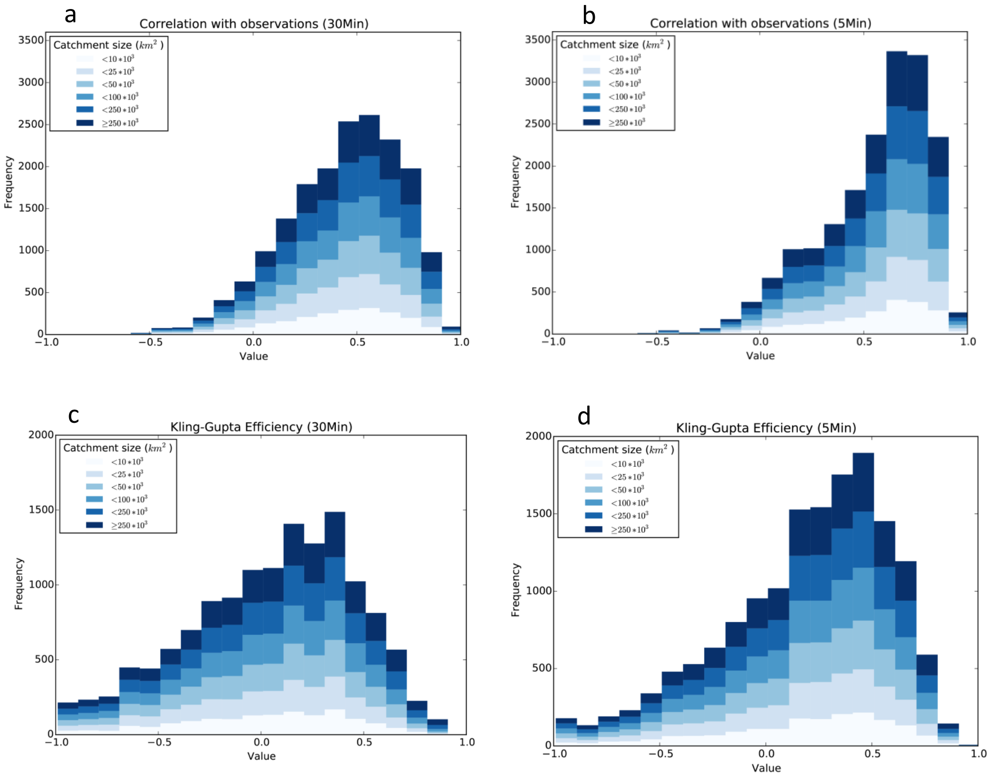

Figure 4. Histograms of validation statistics showing the cross-correlation and Kling-Gupta efficiency (KGE) values for the simulated discharge for the 30 arc-minutes and the 5 arc-minute simulations based on 3597 GRDC discharge stations; a. cross-correlation 30 arc-minute simulation; b. cross-correlation 5 arc-minute simulation; c. KGE 30 arc-minute simulation; d. KGE 5 arc-minute simulation; note: the percentage catchments with KGE < -1 are 21% and 12% for 30 and 5 arc-minutes respectively.

The histograms of the anomaly cross-correlation are shown in Figure 5 The anomaly cross-correlations are generally lower than the cross-correlations, showing that seasonality explains part of the skill in many regions where seasonal variation is dominant when compared to intra-annual or inter-annual variability. Clearly, the 5 arc-minute results are much better than those of the half-degree simulation, indicating a higher skill with regard to capturing extremes and anomalies. Figure 6 shows a map of the difference between the anomaly cross-correlation and the cross-correlation for the 5 arc-minute case. This map shows that there are some regions where the anomaly cross-correlation is better than the cross-correlation (blue colours), e.g. snow-dominated regions in Canada and the Niger basin. These are catchments where the model has difficulty

Geosci. Model Dev. Discuss., https://doi.org/10.5194/gmd-2017-288
Manuscript under review for journal Geosci. Model Dev.
Discussion started: 12 December 2017

reproducing the correct seasonality as a result of errors in snow dynamics (Canada) or groundwater dynamics (Niger). Also, in case of the Niger River, not representing the inner delta flooding and resulting high evaporation may be the cause of poor seasonal timing of discharge.

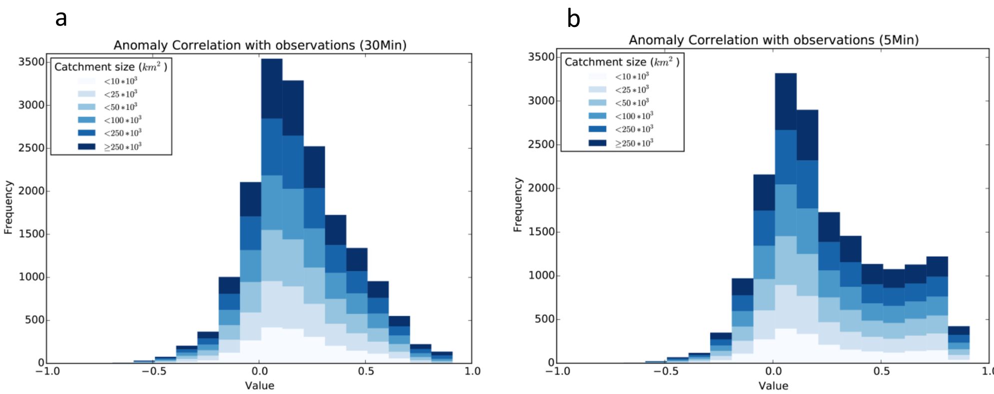

Figure 5. Histograms of validation statistics showing the anomaly cross-correlation for the simulated discharge for the 30 arc-minutes and the 5 arcminute simulations based on 3597 GRDC discharge stations; a. anomaly cross-correlation half arc-degree simulation; b. anomaly cross-correlation 5 arcminute simulation.

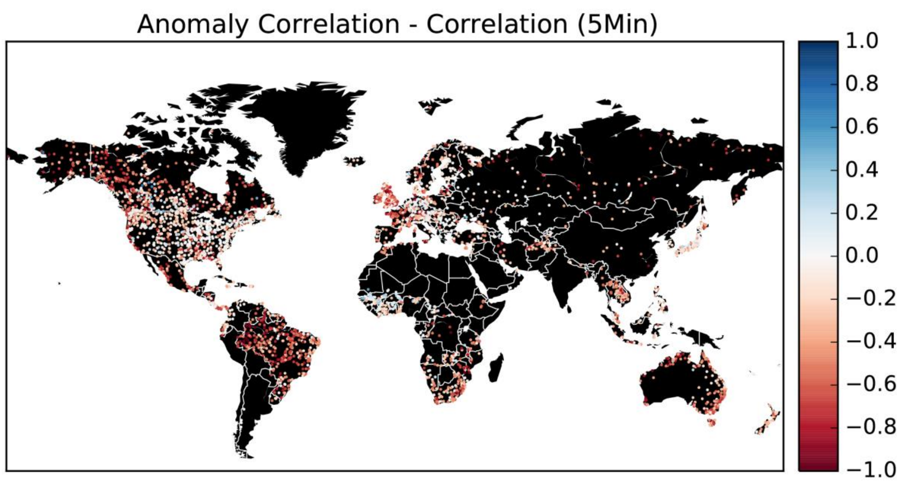

Figure 6. Map showing for the 5 arc-minutes run the difference between the cross-correlation and the anomaly cross-correlation between simulated and observed discharge time series for 3597 GRDC discharge stations; negative values mean that the cross correlation is higher than the anomaly cross-correlation.

Geosci. Model Dev. Discuss., https://doi.org/10.5194/gmd-2017-288
Manuscript under review for journal Geosci. Model Dev.
Discussion started: 12 December 2017

3.4.2 Total water storage

Figure 7 compares the trends in 5 arc-minute simulated total water storage (TWS) with those from GRACE, estimated as the average change in m/year over the period 2003-2015. Generally, the PCR-GLOBWB 2 simulation is able to capture major groundwater depleted regions as suggested by GRACE, such as those in the Central Valley aquifer , the High Plains aquifer, the North China Plain aquifer, as well as parts of the Middle East, Pakistan and India. For these regions, the absolute rates of TWS change (i.e. TWS declines) of PCR-GLOBWB 2 are generally larger, while the spatial pattern in the GRACE map tends to be smoother. This is mainly due to the lower resolution and spatial averaging used in the GRACE product, as well as the fact that the current PCR-GLOBWB 2 simulation does not include lateral groundwater flow between cells. In the polar regions where GRACE estimates mass loss due to melting glaciers and ice sheets, PCR-GLOBWB 2 simulates accumulation as a result of lack of a glacier parameterization. Finally, there are some clear differences over the Amazon and some parts of Africa. A possible explanation are errors in meteorological forcing data, which is not very accurate in these parts, but also problems with the over-estimation of PCR-GLOBWB's groundwater response times in these regions which therefore fail to be sufficiently sensitive to recent changes in terrestrial precipitation.

Further analyses were conducted at the basin-scale resolution, where both TWS time series of PCR-GLOBWB 2 and GRACE *JPL-RL05M* were averaged over a river basins areas map derived from the 5 arc-minute PCR-GLOBWB drainage network. We identified all river basins with sizes larger than 900,000 km^2, which is similar to the GRACE resolution. Smaller river basins were merged to the nearest river basins or grouped together. For the remaining map of large basins, the cross-correlations between PCR-GLOBWB 2 and GRACE basin-average monthly and annual TWS time series were calculated. Monthly cross-correlation provides information about PCR-GLOBWB's ability to correctly time TWS seasonal variability (with a value equal to 1 for perfect timing), while the cross-correlation for annual time series measures inter-annual variability.

The results in Figure 8 show that PCR-GLOBWB 2 is able to capture GRACE's TWS seasonality for most basins around the world, with the exception of some cold regions in high latitudes (e.g. the Yukon River basin, Iceland). This shortcoming is most likely due to the lack of a proper representation of glacier and ice processes in PCR-GLOBWB 2. As expected, the cross-correlation values for inter-annual time series are generally lower than the ones for monthly time series. There are some areas with negative correlation values, such as the Amazon, Niger and Nile river basins. Apart from the uncertainty in the GRACE signal, these deficiencies may be related to errors in model forcing and structural errors such as errors in the groundwater response time and the effects of wetlands that have not been represented sufficiently well.

Geosci. Model Dev. Discuss., https://doi.org/10.5194/gmd-2017-288
Manuscript under review for journal Geosci. Model Dev.
Discussion started: 12 December 2017

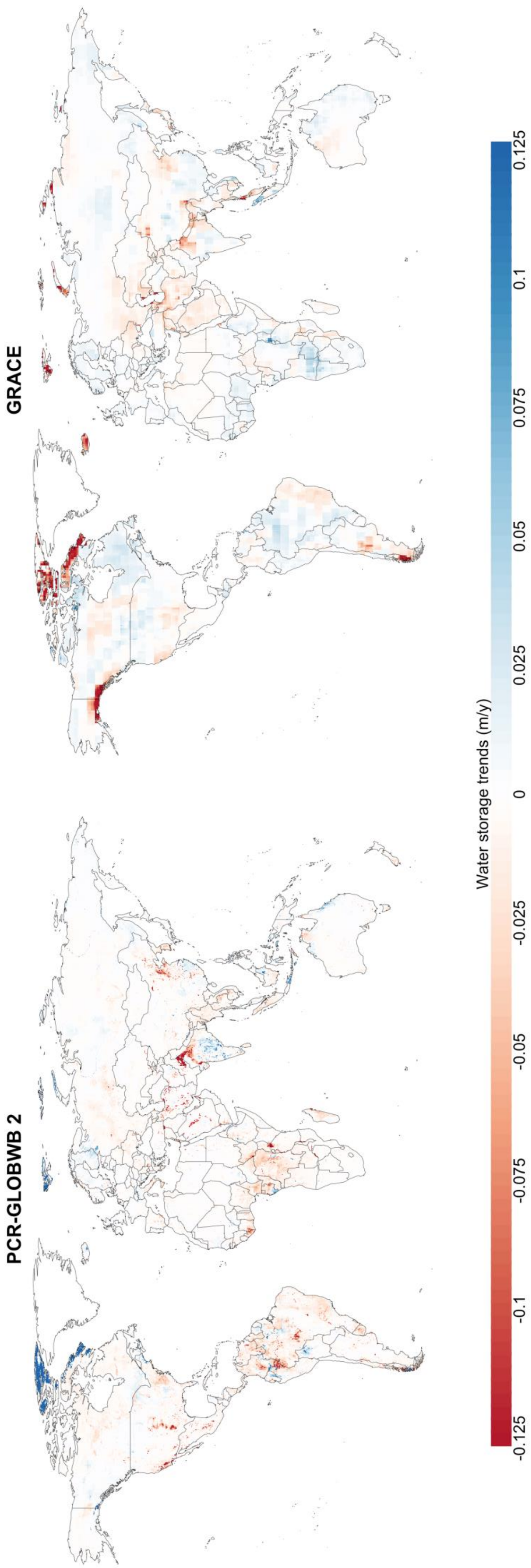

Figure 7. Comparison of PCR-GLOBWB 2 total water storage trends (m/year) with those estimated with GRACE over the period 2003-2015. a. TWS trends simulated with PCR-GLOBWB 2 at 5 arc-minute resolution (~10 km at the equator). Negative values indicate declining TWS (e.g. groundwater depleted regions). b. TWS trends obtained based on the GRACE JPL PL-RL05M Mascon product. The GRACE data were resampled to the resolution of 30 arc-minutes, but they actually represent the 3 x 3 arc-degree (~300 km x 300 km) area, which is the native resolution of the GRACE signal.

Geosci. Model Dev. Discuss., https://doi.org/10.5194/gmd-2017-288
Manuscript under review for journal Geosci. Model Dev.
Discussion started: 12 December 2017

Geoscientific Model Development Discussions

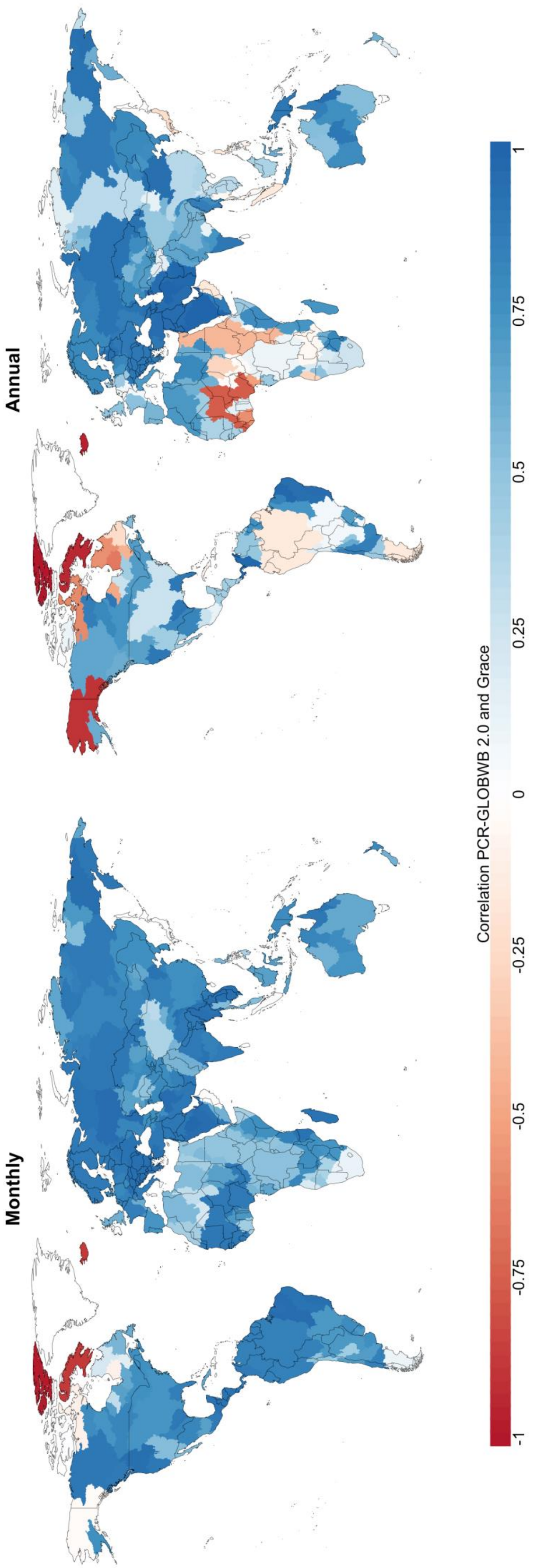

Figure 8. a. Cross-correlation between monthly TWS time series simulated PCR-GLOBWB 2 and the GRACE JPL PL-RL05M Mascon product over the period 2003-2015. b. Comparison of annual TWS series (inter-annual variability). Comparison is only done for the larger basins over 900,000 km^2, conform the 3x3 arc-degree resolution of GRACE.

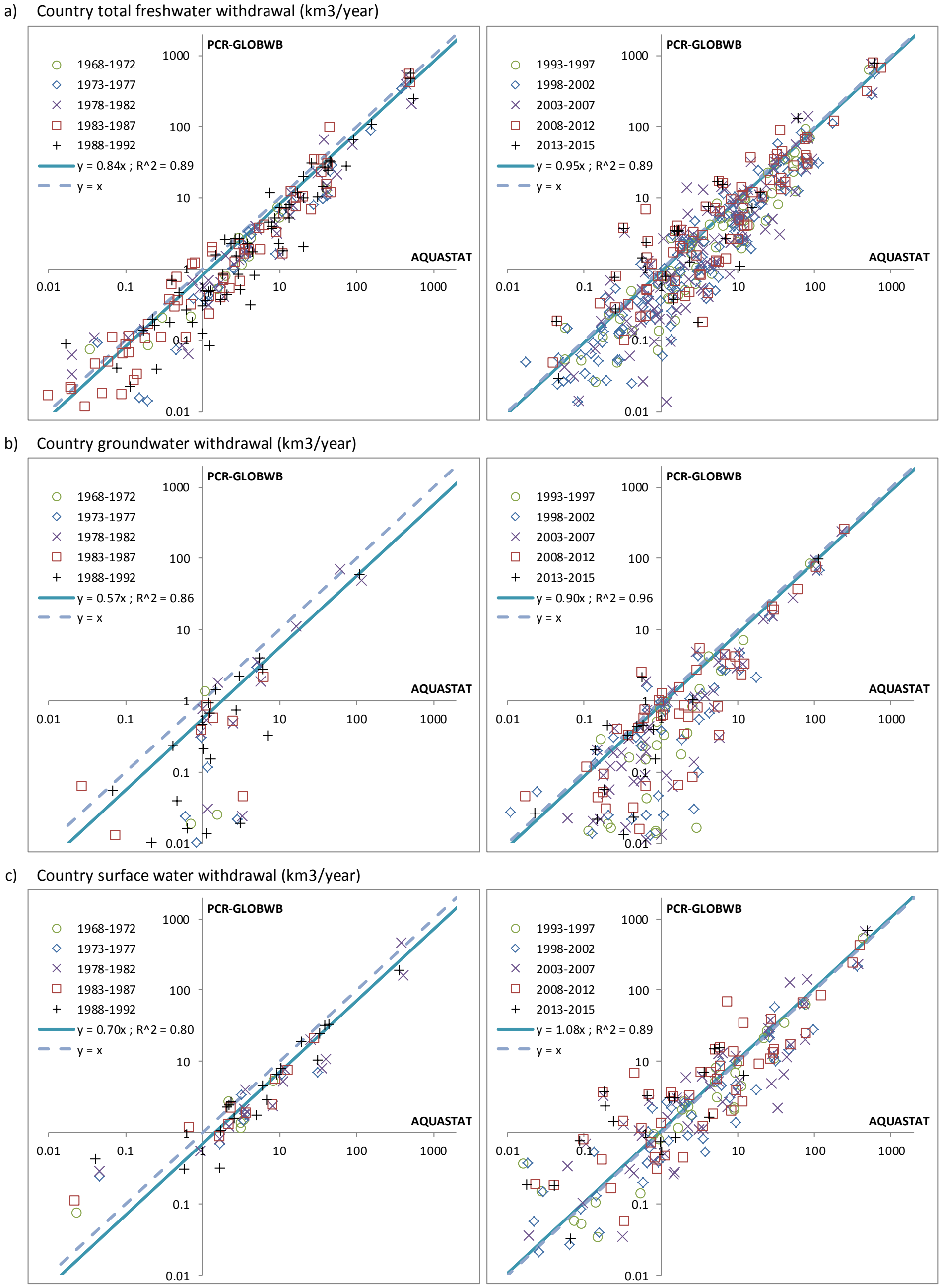

Fig. 9: Country water withdrawal (km^3/year) by source; validation of simulations with PCR-GLOBWB 2 with reported values in AQUASTAT (FAO, 2016) for various periods; a) total water withdrawal; b) groundwater withdrawal; c) surface water withdrawal.

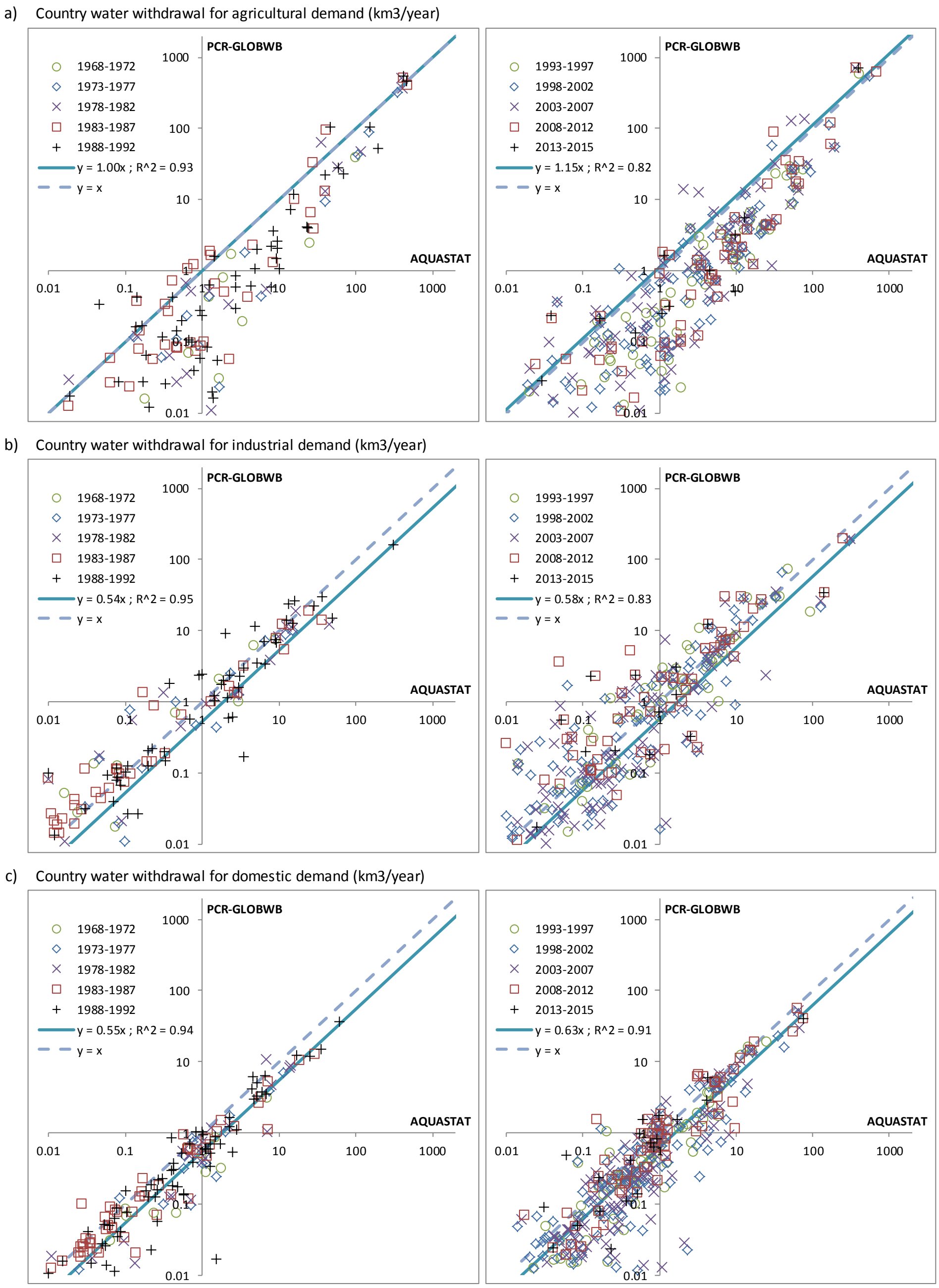

Fig. 10: Country water withdrawal (km³/year) by sector; validation of simulations with PCR-GLOBWB 2 with reported values in AQUASTAT (FAO, 2016) for various periods; a) withdrawal for agricultural demand (irrigation and livestock); b) withdrawal for industrial demand; c) withdrawal for domestic demand.

Geosci. Model Dev. Discuss., https://doi.org/10.5194/gmd-2017-288
Manuscript under review for journal Geosci. Model Dev.
Discussion started: 12 December 2017

3.4.3 Water withdrawal

We compared simulated water withdrawal data from PCR-GLOBWB 2 with reported withdrawal data per country from AQUASTAT (FAO, 2016). The results are shown subdivided per source (Figure 9) and per sector (Figure 10). These figures show that PCR-GLOBWB 2 is able to reproduce reported withdrawal values reasonably well (R^2 between 0.80 and 0.96 and regression slopes between 0.54 and 1.15). There is some underestimation of groundwater withdrawal for the countries with lower withdrawal values. This may be the result of not sufficiently accounting for domestic groundwater withdrawal in populated areas. Also, Figure 10 shows that agricultural water withdrawal is underestimated for countries with smaller withdrawal. A possible cause of this may be the overestimation of irrigation efficiency.

4. Conclusions and future work

We presented the most recent version of the open source global hydrology and water resources model PCR-GLOBWB. This version, PCR-GLOBWB 2, has a global coverage at 5 arc-minute resolution. Apart from the higher resolution, the new model has an integrated water use scheme, i.e. every day sector specific water demand is calculated, resulting in groundwater and surface water withdrawal, water consumption and return flows. Dams and reservoirs from the GranD database (Lehner et al., 2011) are added progressively according to their year of construction. PCR-GLOBWB 2 has been rewritten in Python and uses PCRaster-Python functions (Karssenberg et al., 2007). It has a modular structure, which makes the replacement and maintenance of model parts easier. PCR-GLOBWB 2 can be dynamically coupled to a global 2-layer groundwater model (De Graaf et al., 2017) and a one-way coupling to hydrodynamic models for large-scale inundation modelling (Hoch et al., 2017b) is also available.

Comparing the 5 arc-minute with 30 arc-minute simulations using discharge data we clearly find an improvement in the model performance of the higher resolution model. We find a general increase in correlation, anomaly correlation and KGE, indicating that the higher resolution model is better able to capture the seasonality, hydrological extremes and the general discharge characteristics. Also, PCR-GLOBWB 2 is able to reproduce trends and seasonality in total water storage as observed by GRACE for most river basins. It simulates the hotspots of groundwater decline that around in GRACE as well. Simulated water withdrawal, by source and sector, matches reasonably well with reported water withdrawal from AQUASTAT.

Future work will concentrate on developing a full dynamic (two-way) coupling with hydrodynamic models, developing 5 km and 1 km resolution (or higher) parameterizations of PCR-GLOBWB 2 using scale-consistent parameterizations (e.g. using MPR; Samaniego et al., 2017), incorporating a crop growth model and solving the full surface energy balance. Other foreseeable developments are using the model in probabilistic settings and in data-assimilation frameworks.

5. Code and data availability

PCR-GLOBWB 2 is open source and distributed under the terms of the GNU General Public License version 3, or any later version, as published by the Free Software Foundation. The model code is provided through a Github repository: https://github.com/UU-Hydro/PCR-GLOBWB_model (Sutanudjaja et al., 2017a, https://doi.org/10.5281/zenodo.595656). This keeps users and developers immediately aware of any new revisions. Also, it allows developers to easily collaborate, as they can download a new version, make changes, and suggest and upload the newest revisions. The configuration ini-files for the global 30 arc-minutes and 5-arcminute models and the associated model parameters and input files are provided on https://doi.org/10.5281/zenodo.1045338 (Sutanudjaja et al., 2017b). Development and maintenance of the official version (main branch) of PCR-GLOBWB 2 is conducted at the Department of Physical Geography, Utrecht University. Yet, contributions from external parties are welcome and encouraged. For news on latest developments and papers published based on PCR-GLOBWB 2 we refer to http://www.globalhydrology.nl and for the underlying PCRaster-Python code to http://pcraster.geo.uu.nl.

Acknowledgements

We thank Utrecht University and various grants and projects that directly or indirectly contributed to the development of PCR-GLOBWB 2. The authors are very grateful to all the contributors (as acknowledged in the references) who provided the data sets used in this study. We acknowledge the Netherlands Organisation for Scientific Research (NWO) for the grant that enabled us to use the national super computer Cartesius with the help of SURFsara Amsterdam.

Geosci. Model Dev. Discuss., https://doi.org/10.5194/gmd-2017-288
Manuscript under review for journal Geosci. Model Dev.
Discussion started: 12 December 2017

Geoscientific Model Development Discussions
Open Access
EGU

Appendix

Table A1 - List (non-exhaustive) of state and flux variables defined in PCR-GLOBWB

Description	Symbol	Unit
Interception storage	S_{int}	m
Snow cover/storage in water equivalent thickness (excluding liquid part S_{slq})	S_{swe}	m
Liquid/melt water storage in the snow pack	S_{slq}	m
Upper and lower soil storages	S_1 and S_2	m
Surface water storage (lakes, reservoirs, rivers and inundated water)	S_{wat}	m
groundwater storage (renewable part)	S_3	m
fossil groundwater storage (non-renewable)	S_{nrw}	m
total groundwater storage = $S_3 + S_{nrw}$	S_{gwt}	m
total water storage thickness = $S_{int} + S_{swe} + S_{slq} + S_1 + S_2 + S_{gwt}$	TWS	m
potential evaporation	E_{pot}	$m.day^{-1}$
evaporation flux from the intercepted precipitation	E_{int}	$m.day^{-1}$
evaporation from melt water stored in the snow pack	E_{slq}	$m.day^{-1}$
bare soil evaporation	E_{soil}	$m.day^{-1}$
transpiration from the upper and lower soil stores	T_1 and T_2	$m.day^{-1}$
total land evaporation = $E_{pot} + E_{int} + E_{slq} + E_{soil} + T_1 + T_2$	E_{land}	$m.day^{-1}$
surface water evaporation	E_{wat}	$m.day^{-1}$
total evaporation = $E_{land} + E_{wat}$	E_{tot}	$m.day^{-1}$
direct runoff	Q_{dr}	$m.day^{-1}$
interflow, shallow sub-surface flow	Q_{sf}	$m.day^{-1}$
baseflow, groundwater discharge	Q_{bf}	$m.day^{-1}$
specific runoff from land	Q_{loc}	$m.day^{-1}$
local change in surface water storage	Q_{wat}	$m.day^{-1}$
total specific runoff	Q_{tot}	$m.day^{-1}$
routed channel (surface water) discharge	Q_{chn}	$m^3.sec^{-1}$
net fluxes from the upper to lower soil stores	Q_{12}	$m.day^{-1}$
net groundwater recharge, fluxes from the lower soil to groundwater stores	RCH = Q_{23}	$m.day^{-1}$
surface water infiltration to groundwater	Inf	$m.day^{-1}$
desalinated water withdrawal	W_{sal}	$m.day^{-1}$
surface water withdrawal	W_{wat}	$m.day^{-1}$
renewable groundwater withdrawal	W_3	$m.day^{-1}$
non-renewable groundater withdrawal (groundwater depletion)	W_{nrw}	$m.day^{-1}$
total groundwater withdrawal = $W_3 + W_{nrw}$	W_{gwt}	$m.day^{-1}$
water withdrawal allocated for irrigation purpose	A_{irr}	$m.day^{-1}$
water withdrawal allocated for livestock demand/sector	A_{liv}	$m.day^{-1}$
water withdrawal allocated for agricultural sector = $A_{irr} + A_{liv}$	A_{agr}	$m.day^{-1}$
domestic water withdrawal	A_{dom}	$m.day^{-1}$
industrial water withdrawal	A_{ind}	$m.day^{-1}$

Geosci. Model Dev. Discuss., https://doi.org/10.5194/gmd-2017-288
Manuscript under review for journal Geosci. Model Dev.
Discussion started: 12 December 2017

Geoscientific Model Development Discussions
Open Access
EGU

Table A2 - List of model inputs and parameters

Description	Symbol	Unit	References/sources
Upper and lower soil store parameters:			FAO (2007) soil map; van Beek and Bierkens (2009)
- Soil thickness	Z_1 and Z_2	m	
- Residual soil moisture content	$\theta_{r\text{-}1}$ and $\theta_{r\text{-}2}$	$m^3.m^{-3}$	
- Soil moisture at saturation	$\theta_{s\text{-}1}$ and $\theta_{s\text{-}2}$	$m^3.m^{-3}$	
- Soil water storage capacity per soil layer: $SC = Z / (\theta_s - \theta_r)$	SC_1 and SC_2	m	
- Soil matric suctions at saturation	$\psi_{s\text{-}1}$ and $\psi_{s\text{-}2}$	m	
- Exponent in the soil water retention curve	β_1 and β_2	dimensionless	
- Saturated hydraulic conductivities of upper and lower soil stores	K_1 and K_2	$m.day^{-1}$	
- Total soil water storage capacities = $SC_{upp} + SC_{low}$	W_{max}	m	
Land cover fraction: Land cover areas (including extent of irrigated areas) over cell areas	f_{lcov}	$m^2.m^{-2}$	GLCC v2.0 map (USGS, 1997); Olson (1994a, 1994b); MIRCA2000 dataset (Portmann et al., 2010), FAOSTAT (2012)
Topographical parameters	DEM	m	HydroSHEDS (Lehner et al., 2008); Hydro1k (Verdin and Greenlee, 1996); GTOPO30 (Gesch et al., 1999)
- Cell-average DEM	DEM_{avg}	m	
- Flood plain elevation	DEM_{fpl}	m	
Root fractions per soil layer	Rf_{upp} & Rf_{low}	dimensionless	Canadell et al. (1996); van Beek and Bierkens (2009)
Arno scheme (Todini, 1999; Hagemann and Gates, 2003) exponents defining soil water capacity distribution	β_{arno}	dimensionless	Canadell et al. (1996), Hagemann et al. (1999); Hagemann (2002); van Beek (2008); van Beek and Bierkens (2009)
Ratios of cell-minimum and cell-maximum soil storage to W_{max}	f_{wmin} and f_{wmax}	m	van Beek (2008); van Beek and Bierkens (2009)

Geosci. Model Dev. Discuss., https://doi.org/10.5194/gmd-2017-288
Manuscript under review for journal Geosci. Model Dev.
Discussion started: 12 December 2017

Table A2 - List of model inputs and parameters (continued)

Description	Symbol	Unit	References/sources
Parameters related to phenology			Hagemann et al. (1999); Hagemann (2002); van Beek (2008); van Beek and Bierkens (2009)
- Crop coefficient	K_c	dimensionless	
- Interception capacity	$S_{int\text{-}max}$	m	
- Vegetation cover fraction	C_v	$m^2.m^{-2}$	
Groundwater parameters			GLHYMPS map (Gleeson et al., 2014); van Beek (2008); van Beek and Bierkens (2009)
- Aquifer transmissivity	KD	$m^2.day^{-1}$	
- Aquifer specific yield	Sy	$m^3.m^{-3}$	
- Groundwater recession coefficient	J	day^{-1}	
Meteorological forcing			van Beek (2008); CRU (Harris et al., 2014); ERA40 (Uppala et al., 2005); ERA-Interim (Dee et al., 2011)
- Total precipitation	P	$m.day^{-1}$	
- Atmospheric air temperature	T_{air}	°C or K	
- Reference potential evaporation and transpiration	$E_{ref,pot}$	$m.day^{-1}$	
Others:			
- Non-irrigation sectoral water demand (i.e. livestock, dometic and industrial)		$m.day^{-1}$	Wada et al (2014)
- Desalinated water		$m.day^{-1}$	Wada et al., (2011a); FAO (2016)
- Lakes and reservoirs			GLWD1 (Lehner and Döll, 2004); GranD (Lehner et al., 2011)

Geosci. Model Dev. Discuss., https://doi.org/10.5194/gmd-2017-288
Manuscript under review for journal Geosci. Model Dev.
Discussion started: 12 December 2017

References

Alfieri, L., Burek, P. Dutra, E. Krzeminski, B. Muraro, D. Thielen, J., and Pappenberger F.: GloFAS—Global ensemble streamflow forecasting and flood early warning, Hydrology and Earth System Science, 17, 1161–1175, 2003.

Allen, R.G., Pereira, L.S., Raes, D., and Smith, M.: Crop evaporation: Guidelines for computing crop requirements., UN-FAO, Rome, Italy, 1998.

Bates, P.D., Horritt, M. S., and Fewtrell, T.J.: A simple inertial formulation of the shallow water equations for efficient twodimensional flood inundation modelling, Journal of Hydrology, 38, 33–45, 2010.

Bergström, S.: The HBV model, in: Computer Models in Watershed Hydrology, edited by Singh, V. P., Water Resources Publications, Highlands Ranch, CO, 1995.

Beven, K.J. and Cloke, H.L.: Comment on "Hyperresolution global land surface modeling: Meeting a grand challenge for monitoring Earth's terrestrial water" by Eric F. Wood et al., Water Resources Research, 48, 2012.

Bierkens, M.F.P. and van Beek, L.P.H.: Seasonal Predictability of European Discharge: NAO and Hydrological Response Time, Journal of Hydrometeorology 10, 953–968, 2009.

Bierkens, M.F.P., Bell, V.A., Burek, P., Chaney, N., Condon, L.E., David, C.H., de Roo, A., Döll, P., Drost, N., Famiglietti, J. S., Flörke, M., Gochis, D. J., Houser, P., Hut, R., Keune, J., Kollet, S., Maxwell, R. M., Reager, J. T., Samaniego, L., Sudicky, E., Sutanudjaja, E. H., van de Giesen, N., Winsemius, H., and Wood, E. F.: Hyper-resolution global hydrological modelling: what is next? "Everywhere and locally relevant", Hydrological Processes, 29, 310-320, 2014.

Bosmans, J. H. C., van Beek, L. P. H., Sutanudjaja, E. H., and Bierkens, M. F. P.: Hydrological impacts of global land cover change and human water use, Hydrology and Earth System Science Discussions, https://doi.org/10.5194/hess-2016-621, 2016.

Campbell, G. S.: A simple method for determining unsaturated conductivity from moisture retention data, Soil Science, 117, 311–314, 1974.

Canadell, J., Jackson, R.B., Ehleringer, J.B. et al: Maximum rooting depth of vegetation types at the global scale, Oecologia, https://doi.org/10.1007/BF00329030, 1996.

Candogan Yossef, N., Winsemius, H. Weerts, A. van Beek, L. P. H, and Bierkens, M.F.P.: Skill of a global seasonal streamflow forecasting system, relative roles of initial conditions and meteorological forcing, Water Resources Research 49, 4687–4699, 2013.

Clapp, R. B. and Hornberger, G. M.: Empirical equations for some soil hydraulic properties, Water Resources Research, 14, 601–604, 1978.

Cohen, S., Kettner, A. J., Syvitski, J. P. M., and Fekete, B. A. M.: WBMsed, a distributed global-scale riverine sediment flux model: Model description and validation, Computers in Geosciences, 53, 80–93, 2013.

Dalin, C., Wada, Y., Kastner, T., and M. J. Puma: Groundwater depletion embedded in international food trade, Nature, 543, 700–704, 2017.

Dankers, R., Arnell, N. W., Clark, D. B., Falloon, P. D., Fekete, B. M., Gosling, S. N., Heinke, J., Kim, H., Masaki, Y., Satoh, Y., Stacke, T., Wada, Y., and Wisser, D.: First look at changes in flood hazard in the Inter-Sectoral Impact Model Intercomparison Project ensemble, Proceedings of the National Academy of Sciences, 2013.

De Graaf, I. E. M., van Beek, L. P. H., Wada, Y., and Bierkens, M. F. P.: Dynamic attribution of global water demand to surface water and groundwater resources: Effects of abstractions and return flows on river discharges, Advances in Water Resources 64, 21–33, 2014.

De Graaf, I. E. M., Sutanudjaja, E. H., Van Beek, L. P. H., and Bierkens, M. F. P.: A high-resolution global-scale groundwater model. Hydrology and Earth System Sciences, 19, 823-837, 2015.

De Graaf, I. E., van Beek, L.P.H., Gleeson, T., Moosdorf, N., Schmitz, O., Sutanudjaja, E. H., and Bierkens, M. F. P.: A global-scale two-layer transient groundwater model: Development and application to groundwater depletion. Advances in Water Resources, 102, 53-67, 2017.

Dee, D. P., Uppala, S. M., Simmons, A. J., Berrisford, P., Poli, P., Kobayashi, S., Andrae, U., Balmaseda, M. a., Balsamo, G., Bauer, P., Bechtold, P., Beljaars, a. C. M., van de Berg, L., Bidlot,

Geosci. Model Dev. Discuss., https://doi.org/10.5194/gmd-2017-288
Manuscript under review for journal Geosci. Model Dev.
Discussion started: 12 December 2017

Geoscientific Model Development Discussions
Open Access
EGU

J., Bormann, N., Delsol, C., Dragani, R., Fuentes, M., Geer, a. J., Haimberger, L., Healy, S. B., Hersbach, H., Hólm, E. V., Isaksen, L., Kå llberg, P., Köhler, M., Matricardi, M., McNally, a. P., Monge-Sanz, B. M., Morcrette, J.-J., Park, B.-K., Peubey, C., de Rosnay, P., Tavolato, C., Thépaut, J.-N., and Vitart, F.: The ERA-Interim reanalysis: configuration and performance of the data assimilation system, Quarterly Journal of the Royal Meteorological Society, 137, 553–597, 2011.

Dermody, B. J., van Beek, L. P. H., Meeks, E., Klein Goldewijk, K., Scheidel, W., van der Velde, Y., Bierkens, M. F. P., Wassen, M. J., and Dekker, S. C.: A virtual water network of the Roman world, Hydrology and Earth System Sciences, 18, 5025–5040, http://dx.doi.org/10.5194/hess-18-5025-2014, 2014.

Döll, P. and Siebert, S.: Global modeling of irrigation water requirements, Water Resources Research, 38, 8–1 – 8–10, 2002.

Döll, P., Kaspar, F., and Lehner, B.: A global hydrological model for deriving water availability indicators: model tuning and validation, Journal of Hydrology, 270, 105–134, 2003.

Döll, P., Hoffmann-Dobrev, H., Portmann, F. T., Siebert, S., Eicker, A., Rodell, M., Strassberg, G., and Scanlon, B. R.: Impact of water withdrawals from groundwater and surface water on continental water storage variations, Journal of Geodynamics, 59–60, 143–156, 2012.

Döll, P., Muller Schmied, H., Schuh, Portmann, F. T. and Eicker, A.: Global-scale assessment of groundwater depletion and related groundwater abstractions: Combining hydrological modeling with information from well observations and GRACE satellites, Water Resources Research, 50, 2014.

Doorenbos, J. and Pruitt, W. O.: Crop water requirements, Irrig. Drain. Pap. 24, FAO, Rome, 1977.

Elliott, J., Deryng, D., Müller, C., Frieler, K., Konzmann, M., Gerten, D., Glotter, M., Flörke, M., Wada, Y., Best, N., Eisner, S., Fekete, B. M., Folberth, C., Foster, I., Gosling, S. N., Haddeland, I., Khabarov, N., Ludwig, F., Masaki, Y., Olin, S., Rosenzweig, C., Ruane, A. C., Satoh, Y., Schmid, E., Stacke, T., Tang, Q., and Wisser, D.: Constraints and potentials of future irrigation water availability on agricultural production under climate change, Proceedings of the National Academy of Sciences, 111, 3239–3244, 2013.

Erkens, G. and Sutanudjaja, E. H.: Towards a global land subsidence map, Proc. IAHS, 372, 83-87, https://doi.org/10.5194/piahs-372-83-2015, 2015.

Fekete, B. M. B., Vörösmarty, C. J. C., and Grabs, W.: High-resolution fields of global runoff combining observed river discharge and simulated water balances, Global Biogeochemical Cycles, 16, 10–15, 2002.

Food and Agriculture Organization of the United Nations (FAO): Digital Soil Map of the World, Version 3.6. FAO, Rome, Italy, 2007.

Food and Agriculture Organization of the United Nations (FAO): FAOSTAT statistics database, http://www.fao.org/faostat/en/#home, 2012.

Food and Agriculture Organization of the United Nations (FAO): AQUASTAT database of water-related data. Accessed on [2017-09-15] at: http://www.fao.org/nr/water/aquastat/main/index.stm, 2016.

Gesch, D.B., Verdin, K.L., and Greenlee, S.K.: New Land Surface Digital Elevation Model Covers the Earth: Eos, Transactions, American Geophysical Union, v. 80, no. 6, p. 69–70, 1999.

Gleeson, T., Wada, Y., Bierkens, M. F. P., and van Beek, L. P. H.: Water balance of global aquifers revealed by groundwater footprint, Nature, 488, 197–200, 2012.

Gleeson, T., N. Moosdorf, J. Hartmann, and L. P. H. van Beek: A glimpse beneath earth's surface: GLobal HYdrogeology MaPS (GLHYMPS) of permeability and porosity, Geophys. Res. Lett., 41, 3891–3898, doi:10.1002/2014GL059856, 2014.

Global Soil Data Task: Global Soil Data Products CD-ROM (IGBP-DIS), 2000.

Gosling, S. N. and Arnell, N.W.: Simulating current global river runoff with a global hydrological model: model revisions, validation, and sensitivity analysis, Hydrological Processes, 25, 1129–1145, 2011.

Gupta, H.V., Kling, H., Yilmaz, K.K., and Martinez, G.F.: Decomposition of the mean squared error and NSE performance criteria: Implications for improving hydrological modelling. Journal of Hydrology,377, 80-91, 2009.

Haddeland, I., Heinke, J., Biemans, H., Eisner, S., Flörke, M., Hanasaki, N., Konzmann, M., Ludwig, F., Masaki, Y., Schewe, J., Stacke, T., Tessler, Z. D., Wada, Y., and Wisser, D.: Global water

Geosci. Model Dev. Discuss., https://doi.org/10.5194/gmd-2017-288
Manuscript under review for journal Geosci. Model Dev.
Discussion started: 12 December 2017

Geoscientific Model Development Discussions
Open Access
EGU

resources affected by human interventions and climate change, Proceedings of the National Academy of Sciences, 111, 3251–3256, 2013.

Hagemann, S., Botzet, M., Dümenil, L., and Machenhauer, B.: Derivation of Global GCM Boundary Conditions from 1 Km Land Use Satellite Data, Max-Planck-Institut für Meteorologie, Hamburg, Germany, 1999.

Hagemann, S.: An improved land surface parameter dataset for global and regional climate models, Max- Planck-Institut für Meteorologie, Hamburg, Germany, https://www.mpimet.mpg.de/fileadmin/publikationen/Reports/max_scirep_336.pdf, 2002.

Hagemann, S. and Gates, L.D.: Improving a subgrid runoff parameterization scheme for climate models by the use of high resolution data derived from satellite observations, Climate Dynamics, 21, 349–359, 2003.

Hagemann, S., Botzet, M., Dümenil, L., and Machenhauer, B.: Derivation of Global GCM Boundary Conditions from 1 Km Land Use Satellite Data, Max-Planck-Institut für Meteorologie, Hamburg, Germany, 1999.

Hamon, W.: Computation of Direct Runoff Amounts from Storm Rainfall, IAHS Publ., 63, 52–62, 1963.

Hanasaki, N., Kanae, S., Oki, T., Masuda, K., Motoya, K., Shirakawa, N., Shen, Y., and Tanaka, K.: An integrated model for the assessment of global water resources - Part 1: Model description and input meteorological forcing, Hydrology and Earth System Science, 12, 1007–1025, 2008.

Hanasaki, N., S. Kanae, T. Oki, K. Masuda, K. Motoya, N. Shirakawa, Y. Shen, and K. Tanaka (2008b), An integrated model for the assessment of global water resources - Part 2: Applications and assessments, Hydrology and Earth System Science, 12, 1027–103.

Harbaugh, A.W., Banta, E.R., Hill, M.C., and McDonald, M.G., 2000, MODFLOW-2000, the U.S. Geological Survey modular ground-water model -- User guide to modularization concepts and the Ground-Water Flow Process: U.S. Geological Survey Open-File Report 00-92, 121 p

Harris, I., Jones, P., Osborn, T., and Lister, D.: Updated high-resolution grids of monthly climatic observations - the CRU TS3.10 Dataset, International Journal of Climatology, 34, 623–642, 2014.

Hirabayashi Y., M. Roobavannan, K. Sujan, K. Lisako, Y. Dai, W. Satoshi, K. Hyungjun, and K. Shinjiro (2013), Global flood risk under climate change, Nature Climate Change, 3, 816–821.

Hoch, J.M., Haag, Arjen, van Dam, Arthur, Winsemius, Hessel, van Beek, L.P.H. & Bierkens, M.F.P.: Assessing the impact of hydrodynamics on large-scale flood wave propagation - a case study for the Amazon Basin, Hydrology and Earth System Science, 21, 117-132, 2017a.

Hoch, J.M., Neal, J.C., Baart, F. van Beek, L.P.H., Winsemius, H.C., Bates, P.D., and Bierkens, M.F.P.: GLOFRIM v1.0 – A globally applicable computational framework for integrated hydrological-hydrodynamic modelling. Geoscientific Model Development, 10, 3913-3929, 2017b.

Karssenberg, D., de Jong K., and van der Kwast, J.: Modelling landscape dynamics with Python, International Journal of Geographical Information Science, 21, 483-495, 2007.

Karssenberg, D., Schmitz, O., Salamon, P., de Jong, K., and Bierkens, M. F. P.: A software framework for construction of process-based stochastic spatio-temporal models and data assimilation, Environmental Modelling & Software, 25, 489–502, 2010.

Kauffeldt, A., Wetterhall, F., Pappenberger, F., Salamon, P., and Thielen, J.: Technical review of large-scale hydrological models for implementation in operational flood forecasting schemes on continental level. Environmental Modelling and Software, 75, 68–76, 2016.

Kernkamp, H.W.J., van Dam, A., Stelling, G.S. and de Goede, E.D.: Efficient scheme for the shallow water equations on unstructured grids with application to the Continental Shelf, Ocean Dynamics. 61, 1175–1188, 2011.

Konar, M., Hussein, Z., Hanasaki, N., Mauzerall, D. L., and Rodriguez-Iturbe, I.: Virtual water trade flows and savings under climate change, Hydrology and Earth System Science, 17, 3219–3234, 2013.

Konikow, L. F.: Contribution of global groundwater depletion since 1900 to sea-level rise, Geophysical Research Letters 38, L17401, 1-5, 2011.

Kraijenhoff van de Leur, D.A.: A study of non-steady ground-water flow with special reference to the reservoir-coefficient, De Ingenieur 19, 87-94, 1958.

Lehner, B. and Döll, P.: Development and validation of a global database of lakes, reservoirs and wetlands, Journal of Hydrology 296, 1–22, 2004.

Geosci. Model Dev. Discuss., https://doi.org/10.5194/gmd-2017-288
Manuscript under review for journal Geosci. Model Dev.
Discussion started: 12 December 2017

Lehner, B., Verdin, K., and Jarvis, A.: New global hydrography derived from spaceborne elevation data, Eos (Washington. DC)., 89, DOI: 10.1029/2008EO100001, 2008.

Lehner, B., Reidy Liermann, C., Revenga, C., Vörösmarty, C., Fekete, B., Crouzet, P., Döll, P., Endejan, M., Frenken, K., Magome, J., Nilsson, C., Robertson, J., Rödel, R., Sindorf, N., and Wisser, D.: High- resolution mapping of the world's reservoirs and dams for sustainable river-flow management. Frontiers in Ecology and the Environment, 9 494–502, 2011.

Liang, X., Lettenmaier, D. P., Wood, E. F., and Burges, S. J.: A simple hydrologically based model of land surface water and energy fluxes for general circulation models, Journal of Geophysical Research, 99, 14415–14428, 1994.

Loveland, T. R., Reed, B. C., and Brown, J. F.: Development of a global land cover characteristics database and IGBP DISCover from 1 km AVHRR data, International Journal of Remote Sensing, 21, 1303–1330, 2000.

McDonald, R. I., Weber, K., Padowski, J., Flörke, M., Schneider, C., Green, P. A., Gleeson, T. Eckman, S. Lehner, B. Balk, D., Boucher, T. Grill, G. and Montgomery, M.: Water on an urban planet: Urbanization and the reach of urban water infrastructure. Global Environmental Change, 27, 96-105, 2011.

Murray, F.: On the computation of saturation vapor pressure, IAHS Publ., 6, 203–204, 1967.

New, M., Lister, D., Hulme, M., and Makin, I.: A high-resolution data set of surface climate over global land areas, Climate Research, 21, 1–25, 2002.

Nijssen, B., O'Donnell, G. M., Lettenmaier, D. P., Lohmann, D., and Wood, E. F.: Predicting the Discharge of Global Rivers, Journal of Climate, 14, 3307–3323, 2001.

Oki, T. and Kanae, S.: Global hydrological cycles and world water resources, Science, 313, 1068–1072, 2006.

Olson, J. S.: Global ecosystem framework-definitions, Tech. rep., USGS EROS Data Center Internal Report, Sioux Falls, SD, 1994a.

Olson, J. S.: Global ecosystem framework-translation strategy, Tech. rep., USGS EROS Data Center Internal Report, Sioux Falls, SD, 1994b.

Pappenberger, F., Dutra, E., Wetterhall, F., and Cloke, H.L.: Deriving global flood hazard maps of fluvial floods through a physical model cascade, Hydrology and Earth System Science, 16, 4143–4156, 2012.

Pokhrel, Y. N., Hanasaki, N., Yeh, P. J., Yamada, T. J., Kanae, S., and Oki, T.: Model estimates of sea-level change due to anthropogenic impacts on terrestrial water storage. Nature Geoscience, 5, 389-392, 2012.

Pokhrel, Y. N., Koirala, S. Yeh, P. J.-F., Hanasaki, N., Longuevergne, L., Kanae, S., and Oki, T.: Incorporation of groundwater pumping in a global Land Surface Model with the representation of human impacts, Water Resources Research, 51, 2015.

Portmann, F. T., Siebert, S., and Döll, P.: MIRCA2000-Global monthly irrigated and rainfed crop areas around the year 2000: A new high-resolution data set for agricultural and hydrological modeling, Global Biogeochemical Cycles, GB1011, 1-24, 2010.

Prudhomme, C., Giuntoli, I., Robinson, E. L., Clark, D. B., Arnell, N. W., Dankers, R., Fekete, B. M., Franssen, W., Gerten, D., Gosling, S. N., Hagemann, S., Hannah, D. M., Kim, H., Masaki, Y., Satoh, Y., Stacke, T., Wada, Y., and Wisser, D.: Hydrological droughts in the 21st century, hotspots and uncertainties from a global multimodel ensemble experiment, Proceedings of the National Academy of Sciences, 111, 3262–3267, 2013.

Rodell, M.; Beaudoing, H. K.; L'Ecuyer, T. S.; Olson, W. S.; Famiglietti, J. S.; Houser, P. R.; Adler, R.; Bosilovich, M. G.; Clayson, C. A.; Chambers, D.; Clark, E.; Fetzer, E. J.; Gao, X.; Gu, G.; Hilburn, K.; Huffman, G. J.; Lettenmaier, D. P.; Liu, W. T.; Robertson, F. R.; Schlosser, C. A.; Sheffield, J.; Wood, E. F.: The Observed State of the Water Cycle in the Early Twenty-First Century. Journal of Climate, 28, 8289-8318, 2012.

Rost, S., Gerten, D., and Heyder, U.: Human alterations of the terrestrial water cycle through land management, Advances in Geosciences, 18, 43–50, 2008.

Samaniego, L. Kumar, R., Thober, S., Rakovec, O., Zink, M., Wanders, N., Eisner, S., Müller Schmied, H., Sutanudjaja, E.H., Warrach-Sagi K., and Attinger, S.: Toward seamless hydrologic predictions across spatial scales, Hydrology and Earth System Science, 21, 4323-4346, 2017.

Geosci. Model Dev. Discuss., https://doi.org/10.5194/gmd-2017-288
Manuscript under review for journal Geosci. Model Dev.
Discussion started: 12 December 2017

Geoscientific Model Development Discussions

Savenije, H. H. G.: The importance of interception and why we should delete the term evaporation from our vocabulary, Hydrological Processes, 18, 1507–1511, 2004.

Schewe, J., Heinke, J., Gerten, D., Haddeland, I., Arnell, N. W., Clark, D. B., Dankers, R., Eisner, S., Fekete, B. M., Colón-González, F. J., Gosling, S. N., Kim, H., Liu, X., Masaki, Y., Portmann, F. T., Satoh, Y., Stacke, T., Tang, Q., Wada, Y., Wisser, D., Albrecht, T., Frieler, K., Piontek, F., Warszawski, L., and Kabat, P.: Multimodel assessment of water scarcity under climate change, Proceedings of the National Academy of Sciences, 111, 3245–3250, 2013.

Sheffield, J., Wood, E. F., and Munoz-Arriola, F.: Long-Term Regional Estimates of Evaporation for Mexico Based on Downscaled ISCCP Data, Journal of Hydrometeoroly, 11, 253–275, 2010.

Siebert, S., Döll, P., Hoogeveen, J., Faures, J.-M., Frenken, K., and Feick, S.: Development and validation of the global map of irrigation areas, Hydrology and Earth System Science, 9, 535–547, 2005.

Siebert, S. and Döll, P.: Quantifying blue and green virtual water contents in global crop production as well as potential production losses without irrigation, Journal of Hydrology, 384, 198–217, 2010.

Siebert, S., Burke, J., Faures, J. M., Frenken, K., Hoogeveen, J., Döll, P., and Portmann, F. T.: Groundwater use for irrigation–a global inventory. Hydrology and Earth System Sciences, 14(10), 1863-1880, 2010.

Siebert, S., Henrich, V., Frenken, K., Burke, J.: Update of the Global Map of Irrigation Areas to version 5. Project report, 178 p., 2013.

Sloan, P.G. and I.D. Moore: Modeling subsurface stormflow on steeply sloping forested watersheds, Water Resources Research 20, 1815–1822, 1984.

Sperna Weiland, F. C., van Beek, L. P. H., Kwadijk, J. C. J., and Bierkens, M. F. P.: Global patterns of change in discharge regimes for 2100, Hydrology and Earth System Science, 16, 1047–1062, 2012.

Sterling, S. M., Ducharne, A., and Polcher, J.: The impact of global land-cover change on the terrestrial water cycle, Nature Climate Change, 3, 385–390, 2013.

Sutanudjaja, E. H., van Beek, L. P. H., de Jong, S. M., van Geer, F. C., and Bierkens, M. F. P.: Large-scale groundwater modeling using global datasets: a test case for the Rhine-Meuse basin, Hydrology and Earth System Science, 15, 2913–2935, 2011.

Sutanudjaja, E. H., van Beek, L. P. H., de Jong, S. M., van Geer, F. C., and Bierkens, M. F. P.: Calibrating a large-extent high-resolution coupled groundwater-land surface model using soil moisture and discharge data, Water Resources Research, 50, 687–705, 2014.

Sutanudjaja, E.H., van Beek, Rens, Wanders, Niko, Wada, Yoshihide, Bosmans, Joyce, Drost, Niels, van der Ent, Ruud, de Graaf, Inge, Hoch, Jannis, de Jong, Kor, Karssenberg, Derek, López López, Patricia, Peßenteiner, Stefanie, Schmitz, Oliver, Straatsma, Menno, Vannametee, Ekkamol, Wisser, Dominik and Bierkens, Marc: PCR-GLOBWB_model: PCR-GLOBWB version v2.1.0_beta_1, , doi:10.5281/zenodo.247139, 2017a.

Sutanudjaja, E.H., van Beek, Rens, Wanders, Niko, Wada, Yoshihide, Bosmans, Joyce, Drost, Niels, van der Ent, Ruud, de Graaf, Inge, Hoch, Jannis, de Jong, Kor, Karssenberg, Derek, López López, Patricia, Peßenteiner, Stefanie, Schmitz, Oliver, Straatsma, Menno, Vannametee, Ekkamol, Wisser, Dominik and Bierkens, Marc: PCR-GLOBWB 2 input files version 2017_11_beta_1, doi:10.5281/zenodo.1045339, 2017b.

The Global Runoff Data Centre (GRDC): The Global Runoff Database and River Discharge Data. 56068 Koblenz, Germany. Data were requested from http://www.bafg.de/GRDC and made available for us on 17 April 2014, 2014.

Todini, E.: The ARNO rainfall-runoff model, Journal of Hydrology, 175, 339–382, 1996.

Uppala, S.M. et al.: The ERA-40 re-analysis, Quarterly Journal of the Royal Meteorological Society 131, 2961–3012, 2005.

USGS EROS Data Center: HYDRO1k Elevation Derivative Database, LP DAAC: http://edcdaac.usgs.gov/gtopo30/hydro/, 2006.

Van Beek, L. P. H.: Forcing PCR-GLOBWB with CRU data, Tech. rep., Department of Physical Geography, Utrecht University, Utrecht, The Netherlands, http://vanbeek.geo.uu.nl/suppinfo/vanbeek2008.pdf, 2008.

Van Beek, L. P. H. and Bierkens, M. F. P.: The Global Hydrological Model PCR-GLOBWB: Conceptualization, Parameterization and Verification, Tech. rep., Department of Physical

Geosci. Model Dev. Discuss., https://doi.org/10.5194/gmd-2017-288
Manuscript under review for journal Geosci. Model Dev.
Discussion started: 12 December 2017

Geography, Utrecht University, Utrecht, The Netherlands, http://vanbeek.geo.uu.nl/suppinfo/vanbeekbierkens2009.pdf, 2009.

Van Beek, L. P. H., Wada, Y., and Bierkens, M. F. P.: Global monthly water stress: 1. Water balance and water availability, Water Resources Research, 47, W07 517, 2011.

Van Beek, L. P. H., Eikelboom, T., van Vliet, M. T. H. and Bierkens, M. F. P.: A physically based model of global freshwater surface temperature, Water Resources Research, 48, W09530, doi:10.1029/2012WR011819, 2012.

Van Vliet, M. T. H., Yearsley, J. R. F. Ludwig, Vögele, S, Lettenmaier, D.P. and Kabat, P.: Vulnerability of US and European electricity supply to climate change, Nature Climate Change, 2, 676–681, 2012.

Verdin, K.L., and Greenlee, S.K.,: Development of continental scale digital elevation models and extraction of hydrographic features. In: Proceedings, Third International Conference/Workshop on Integrating GIS and Environmental Modeling, Santa Fe, New Mexico, January 21-26, 1996. National Center for Geographic Information and Analysis, Santa Barbara, California, 1996.

Vörösmarty, C. J., Leveque, C., and Revenga, C.: Millennium Ecosystem Assessment Volume 1: Conditions and Trends, chap. 7: Freshwater ecosystems, Island Press, Washington DC, USA, 165–207, 2005.

Wada, Y., van Beek, L. P. H., van Kempen, C. M., Reckman, J. W. T. M., Vasak, S., and Bierkens, M. F. P.: Global depletion of groundwater resources, Geophys. Res. Lett., 37, L20 402, 1-5, 2010.

Wada, Y., van Beek, L. P. H., Viviroli, D., Dürr, H. H., Weingartner, R., and Bierkens, M. F. P.: Global monthly water stress: 2. Water demand and severity of water stress, Water Resources Research, 47, W07 518, 1-17, 2011a.

Wada, Y., van Beek, L. P. H. and Bierkens, M.F P.: Modelling global water stress of the recent past: On the relative importance of trends in water demand and climate variability, Hydrology and Earth System Science, 15, 3785–3808, 2011b.

Wada, Y., van Beek, L. P. H., and Bierkens, M. F. P.: Nonsustainable groundwater sustaining irrigation: A global assessment, Water Resources Research, 48,1-18, 2012a.

Wada, Y., van Beek, L. P. H., Sperna Weiland, F. C., Chao, B. F., Wu, Y.-H., and Bierkens, M. F. P.: Past and future contribution of global groundwater depletion to sea-level rise, Geophysical Research Letters, 39, L09402, 1-6, 2012b.

Wada, Y., van Beek, L.P.H., Wanders N., and Bierkens, M.F.P.: Human water consumption intensifies hydrological drought worldwide. Environmental Research Letters 8, 034036, 2013.

Wada, Y., Wisser, D., and Bierkens, M. F. P.: Global modeling of withdrawal, allocation and consumptive use of surface water and groundwater resources, Earth System Dynamics, 5, 15–40, 2014.

Wada, Y., and M. F. P. Bierkens: Sustainability of global water use: past reconstruction and future projections, Environmental. Research Letters, 9, 104003, 2014.

Wada, Y., de Graaf, I.E.M., and van Beek, L.P.H.: High-resolution modeling of human and climate impacts on global water resources, Journal of Advances in Modeling Earth Systems, 8, 735–763, 2016.

Wanders, N., Wada, Y., and Van Lanen, H. A. J.: Global hydrological droughts in the 21st century under a changing hydrological regime. Earth System Dynamics, 6, 1–15, 2015

Wanders, N. and Wada, Y.: Decadal predictability of river discharge with climate oscillations over the 20th and early 21st century, Geophysical Research Letters, 42, 10689-10695, 2015

Wanders, N. and Wada, Y.: Human and climate impacts on the 21st century hydrological drought. Journal of Hydrology, 526, 208-220, 2016

Ward, P. J., Jongman, B., Sperna-Weiland, F., Bouwman, A., van Beek, L. P. H., Bierkens, M. F. P., Ligtvoet, W., and Winsemius, H.C.: Assessing flood risk at the global scale: Model setup, results, and sensitivity, Environmental Research Letters, 8, 044019, 2013.

Watkins, M. M., Wiese, D. N., Yuan, D.-N., Boening, C. and Landerer, F.W.: Improved methods for observing Earth's time variable mass distribution with GRACE using spherical cap mascons, Journal of Geophysical Research - Solid Earth, 120, 2648–2671, 2015.

Wesseling, C. G., Karssenberg, D., van Deursen, W. P. A., and Burrough, P. A.: Integrating dynamic environmental models in GIS: The development of a Dynamic Modelling language, Transaction in GIS, 1, 40–48, 1996.

Geosci. Model Dev. Discuss., https://doi.org/10.5194/gmd-2017-288
Manuscript under review for journal Geosci. Model Dev.
Discussion started: 12 December 2017

Geoscientific Model Development
Discussions
Open Access

Wiese. D.N.: GRACE monthly global water mass grids NETCDF RELEASE 5.0. Ver. 5.0. PO.DAAC, CA, USA. Dataset accessed [2017-09-15] at http://dx.doi.org/10.5067/TEMSC-OCL05, 2015.

Wiese, D. N., Landerer, F. W., and Watkins M. M.: Quantifying and reducing leakage errors in the JPL RL05M GRACE mascon solution, Water Resources Research, 52, 7490–7502, 2016.

Winsemius, H. C., Van Beek, L. P. H., Jongman, B., Ward, P. J., and Bouwman, A.: A framework for global river flood risk assessments, Hydrology and Earth System Science, 17, 1871–1892, 2013.

Winsemius, H. C., Aerts, J. C., van Beek, L. P., Bierkens, M. F.P., Bouwman, A., Jongman, B., Kwadijk, J. C., Ligtvoet, W., Lucas, P. L., van Vuuren, D. P., and Ward, P.J.: Global drivers of future river flood risk, Nature Climate Change, 6, 381–385, 2016.

Wisser, D., Fekete, B. M., Vörösmarty, C. J., and Schumann, A. H.: Reconstructing 20th century global hydrography: a contribution to the Global Terrestrial Network- Hydrology (GTN-H), Hydrology and Earth System Sciences, 14, 1–24, 2010.

Wood, E. F., Roundy, J. K., Troy, T. J., van Beek, L. P. H., Bierkens, M. F. P., Blyth, E., de Roo, A., Döll, P., Ek, M., Famiglietti, J., Gochis, D., van de Giesen, N., Houser, P., Jaffé, P. R., Kollet, S., Lehner, B., Lettenmaier, D. P., Peters-Lidard, C., Sivapalan, M., Sheffield, J., Wade, A., and Whitehead, P.: Hyperresolution global land surface modeling: Meeting a grand challenge for monitoring Earth's terrestrial water, Water Resources Research, 47, W05 301, 1-10, 2011.